

Available online at [www.sciencedirect.com](http://www.sciencedirect.com)

SCIENCE @ DIRECT®

EPSL

Earth and Planetary Science Letters xx (2006) xxx–xxx

[www.elsevier.com/locate/epsl](http://www.elsevier.com/locate/epsl)

## Cenozoic intraplate volcanism on New Zealand: Upwelling induced by lithospheric removal

K. Hoernle <sup>a,\*</sup>, J.D.L. White <sup>b</sup>, P. van den Bogaard <sup>c</sup>, F. Hauff <sup>c</sup>, D.S. Coombs <sup>b</sup>,  
R. Werner <sup>d</sup>, C. Timm <sup>c</sup>, D. Garbe-Schönberg <sup>e</sup>, A. Reay <sup>b</sup>, A.F. Cooper <sup>b</sup>

<sup>a</sup> IFM-GEOMAR Leibniz Institute for Marine Sciences at the Christian Albrechts University of Kiel, Wischhofstr. 1-3, D-24148 Kiel, Germany

<sup>b</sup> Geology Department, University of Otago, PO Box 56, Dunedin 9015, New Zealand

<sup>c</sup> IFM-GEOMAR Leibniz Institute for Marine Sciences, Wischhofstr. 1-3, D-24148 Kiel, Germany

<sup>d</sup> Tethys Geoconsulting GmbH, Wischhofstraße 1-3, 24148 Kiel, Germany

<sup>e</sup> Institut für Geowissenschaften, Christian Albrechts University of Kiel, Ludwig-Meyn-Strasse 10, 24118 Kiel, Germany

Received 21 December 2005; received in revised form 31 May 2006; accepted 1 June 2006

Editor: R.W. Carlson

### Abstract

Diffuse intraplate volcanism spanning the Cenozoic on the North, South, Chatham, Auckland, Campbell and Antipodes Islands of New Zealand has produced quartz tholeiitic to basanitic/nephelinitic (including their differentiates) monogenetic volcanic fields and large shield volcanoes. New <sup>40</sup>Ar/<sup>39</sup>Ar ages, combined with published age data, show no correlations among age, location or composition of the volcanoes. Continuous volcanism in restricted areas over long time periods, and a lack of volcanic age progressions in the direction and at the rate of plate motion, are inconsistent with a plume origin for the intraplate volcanism. Although localized extension took place during some episodes of volcanic activity, the degree of extension does not correlate with erupted volumes or compositions. Major and trace element data suggest that the silica-poor volcanic rocks (primarily basanites) were derived through low degrees of partial melting at deeper depths than the more silica-rich volcanic rocks (alkali basalts and tholeiites) and that all melts were produced from ocean island basalt (OIB)-type sources, containing garnet pyroxenite or eclogite. The Sr–Nd–Pb isotope data indicate that the silica-poor rocks were derived from high time-integrated U/Pb (HIMU)-type sources and the silica-rich rocks from more enriched mantle (EM)-type sources, reflecting greater interaction with lithosphere modified by subduction beneath Gondwana. The first-order cause of melting is inferred to be decompression melting in the garnet stability field of upwelling asthenosphere, triggered by removal (detachment) of different parts of the subcontinental lithospheric keel throughout the Cenozoic. In some cases, large thicknesses of keel were removed and magmatism extended over many millions of years. Decompression melting beneath a thick craton generates melts that are likely to be similar to those from the base of the mid-ocean-ridge melting column. At mid-ocean ridges, however, these melts never reach the surface in their pure form due to the swamping effect of larger-degree melts formed at shallower depths. Different volcanic styles in part reflect the mode of removal, and size and shape of detached parts of the lithospheric keel. Removal of continental lithospheric mantle could be an important process for explaining the origin of diffuse igneous provinces on continental lithosphere.

© 2006 Published by Elsevier B.V.

**Keywords:** intraplate volcanism; continental diffuse igneous province; New Zealand; <sup>40</sup>Ar/<sup>39</sup>Ar ages; geochemistry; lithospheric removal/detachment

\* Corresponding author. Tel.: +49 431 6002642; fax: +49 431 6002924.

E-mail address: [khoernle@ifm-geomar.de](mailto:khoernle@ifm-geomar.de) (K. Hoernle).

## 38 1. Introduction

39 Since the plate tectonic model achieved wide accep-  
 40 tance, intraplate volcanism has been primarily attributed  
 41 to mantle plumes [1], which now are generally pre-  
 42 sumed to represent cylindrical regions of mantle up-  
 43 welling (~100–300 km in diameter) from a thermal  
 44 boundary layer such as the core/mantle boundary. The  
 45 mantle plume model is, however, being increasingly  
 46 questioned, leading to the global “Great Plume Debate”  
 47 (e.g. <http://www.mantleplumes.org>). The major alterna-  
 48 tive to the plume model for intraplate volcanism in

49 continental areas is decompression melting of upwelling  
 50 shallow mantle that results from tectonic thinning of the  
 51 lithosphere (e.g. [2]). Neither of these models, however,  
 52 can adequately explain diffuse volcanism known from  
 53 many continental areas globally.

54 New Zealand’s South Island has been the site of nume-  
 55 rous temporally and spatially dispersed episodes of in-  
 56 traplate volcanism throughout the Cenozoic (Fig. 1). This  
 57 intraplate volcanism has produced: 1) scattered, low-  
 58 volume alkalic dikes (e.g. Alpine Dikes) and monogenetic  
 59 volcanic fields (e.g. Waipiata volcanics), 2) several cubic  
 60 kilometers of tholeiitic volcanic rocks erupted from

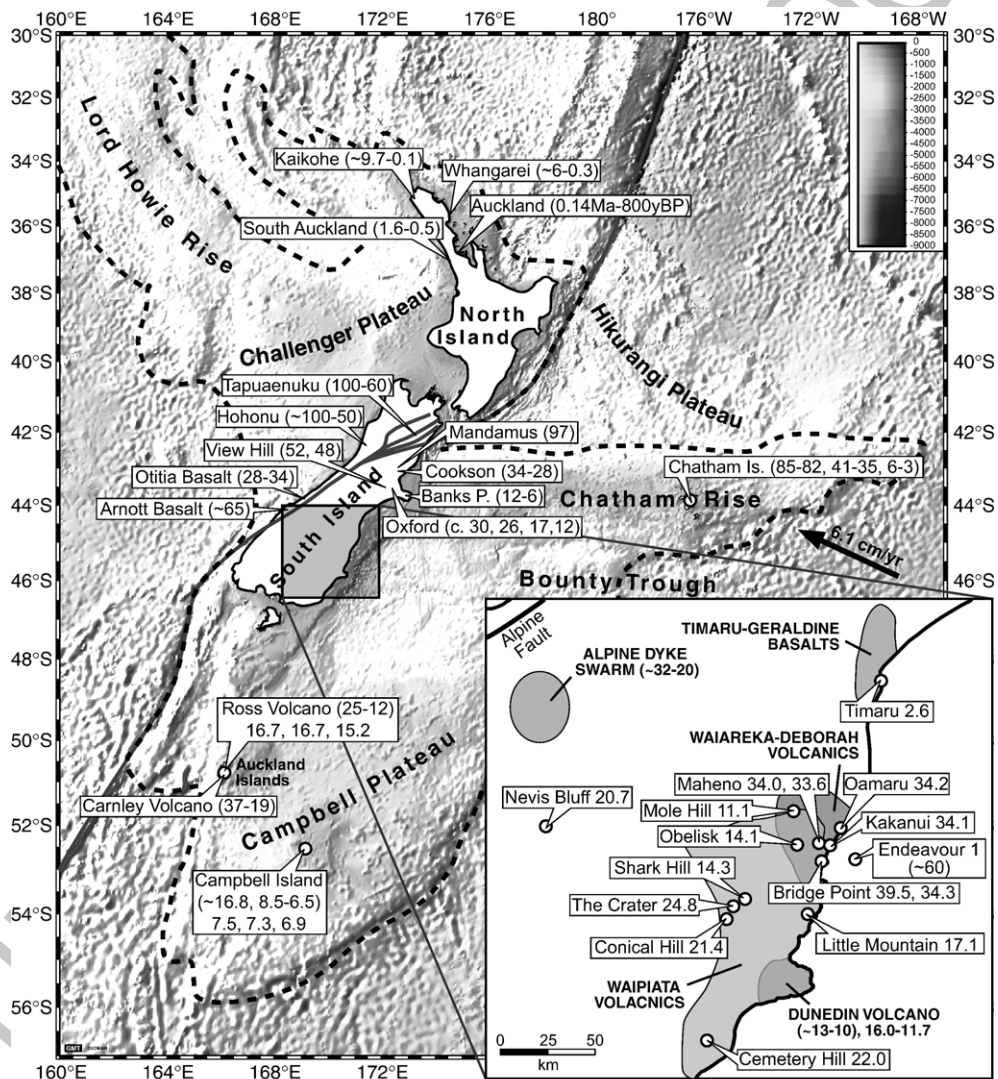


Fig. 1. Overview map of the Zealandia micro-continent, summarizing the published age data. Bathymetry is based on satellite altimetry and ship depth soundings [71]. Shading (see key in upper right hand corner) refers to water depth in meters. Inset: Blow-up map of Otago and southern Canterbury, South Island, showing the  $^{40}\text{Ar}/^{39}\text{Ar}$  age data for intraplate volcanism from this study. Numbers beside the named localities give ages in Ma. Those without parentheses are Ar/Ar ages from this study (Table 1); those within parentheses are K/Ar and other dates from publications referred to in the text. Plate motion vector is from [43].

Sample no.	Dated material	Dating method	Age±2 $\sigma$ (Ma)	MSWD <sup>a</sup>	% <sup>39</sup> Ar in plateau
<i>Otago: Waiareka–Deborah</i>					
LSI7	Matrix	Step heating	39.5±1.8	0.83	69
OU47055	Glass	Step heating	34.2±0.4	0.84	100
	Glass	Single fusions	34.3±0.9	3.31	( <i>N</i> <sup>b</sup> =13)
OU54929	Matrix	Step heating	34.0±0.6	0.86	55
KK1	Hornblende	Step heating	33.7±0.3	1.40	87
	Hornblende	Single fusions	34.1±0.1	0.87	( <i>N</i> <sup>b</sup> =14)
OU55008	Matrix	Single fusions	33.6±1.8	–	( <i>N</i> <sup>b</sup> =2)
MSI99A	Matrix	Step heating	34.3±0.5	1.10	47
<i>Otago: Alpine Dike Outlier</i>					
OU42071	Matrix	Single fusions	20.7±0.4	1.09	( <i>N</i> <sup>b</sup> =12)
<i>Otago: Waipiata</i>					
LSI4	Matrix	Step heating	24.8±0.6	0.89	85
OU54935	Matrix	Step heating	22.0±0.3	1.15	67
LSI1	Matrix	Step heating	21.4±0.4	0.92	87
OU66573	Matrix	Step heating	17.1±0.5	0.57	67
	Matrix duplicate	Step heating	17.0±0.5	0.93	84
LSI3	Matrix	Step heating	14.4±0.2	0.53	64
	Matrix duplicate	Step heating	14.2±0.2	0.55	81
OU55018	Feldspar	Step heating	14.1±0.6	1.50	61
MSI76	Matrix	Step heating	11.1±0.6	1.60	72
<i>Otago: Dunedin Volcano</i>					
LSI23	Matrix	Step heating	16.0±0.4	0.66	63
LSI22	Matrix	Step heating	14.6±0.4	0.53	78
OU22855	Matrix	Step heating	13.0±0.6	0.25	67
	Matrix	Single fusions	13.2±0.5	0.95	( <i>N</i> <sup>b</sup> =13)
MSI184	Hornblende	Step heating	13.0±0.2	1.04	84
UM peperite	Glass	Step heating	11.7±0.1	0.85	71

Table 1 (continued)

Sample no.	Dated material	Dating method	Age±2 $\sigma$ (Ma)	MSWD <sup>a</sup>	% <sup>39</sup> Ar in plateau
<i>Canterbury: Timaru</i>					
OU33298	Glass	Single fusions	2.6±0.4	1.14	( <i>N</i> <sup>b</sup> =35)
<i>Campbell Plateau: Auckland Island</i>					
OU19560	Matrix	Step heating	16.7±1.2	0.65	52
OU19577	Matrix	Step heating	16.7±0.1	0.53	99
OU19606	Matrix	Step heating	15.2±0.3	1.30	46
<i>Campbell Plateau: Campbell Island</i>					
OU36173	Matrix	Step heating	7.3±0.3	1.30	70
	Feldspar	Step heating	6.6±0.6	1.50	100
OU36174	Matrix	Step heating	6.94±0.05	1.40	79
OU36176	Feldspar	Single fusion	7.5±0.3	0.67	( <i>N</i> <sup>b</sup> =15)

<sup>a</sup> MSWD = Mean Squared Weighted Deviates.<sup>b</sup> *N* = Number of Single Fusion Analyses.

spatially and temporally restricted centers (e.g. Timaru and Geraldine lava flows), 3) closely related tholeiitic and alkalic volcanism (e.g. Banks Peninsula [3]), 4) large composite shield volcanoes (e.g. Dunedin and Campbell Island volcanoes) having edifice volumes of up to 1200 km<sup>3</sup>, which can occur as clusters (e.g. Auckland Islands and Banks Peninsula shield volcanoes). The cause of this Cenozoic melting, which produced magmas ranging from highly SiO<sub>2</sub>-undersaturated (e.g. basanitic and nephelinitic) to quartz tholeiitic and their more evolved differentiates, is poorly understood and controversial. In order to explain the widely dispersed Cenozoic intraplate volcanism on the (mostly submerged) New Zealand micro-continent (Fig. 1), here referred to as Zealandia, with the plume model, many dozens of small plumes (plume swarm) or a diffuse megaplume are required. There is, however, no geophysical (e.g. seismic tomographic) evidence for plume-like structures beneath New Zealand (e.g. [4]). In addition, <sup>3</sup>He/<sup>4</sup>He isotope ratios of fluid inclusions in mantle xenocrysts and basalt phenocrysts from the South Island appear to support derivation of the intraplate magmas from degassed upper mid-ocean-ridge basalt (MORB)-type mantle beneath New Zealand [5].

Many often contradictory models have been proposed to explain the Cenozoic intraplate volcanism on Zealandia. Major continental rifting associated with the

t1.35

t1.36

t1.38

t1.39

t1.41

t1.42

t1.43

t1.44

t1.46

t1.47

t1.48

t1.49

t1.50

t1.51

61

62

63

64

65

66

67

68

69

70

71

72

73

74

75

76

77

78

79

80

81

82

83

84

85

86

87

t2.1 Table 2

t2.2 Sr–Nd–Pb isotope data for Cenozoic intraplate volcanic rocks from New Zealand

t2.3	Sample no.	$^{86}\text{Sr}/^{87}\text{Sr}$	$2\sigma$	$^{143}\text{Nd}/^{144}\text{Nd}$	$2\sigma$	$^{206}\text{Pb}/^{204}\text{Pb}$	$2\sigma$	$^{207}\text{Pb}/^{204}\text{Pb}$	$2\sigma$	$^{208}\text{Pb}/^{204}\text{Pb}$	$2\sigma$
	<i>Otago: Waiareka–Deborah</i>										
t2.5	LSI7*	0.703380	4	0.512849	3	18.999	1	15.628	1	38.735	2
t2.6	OU47055	0.703266	7	0.512844	8	19.118	1	15.617	1	38.763	2
t2.7	OU54929	0.703210	7	0.512861	6	19.246	5	15.627	4	38.854	9
t2.8	OU54929					19.248	2	15.636	1	38.888	4
t2.9	OU55008	0.703419	6	0.512839	9	19.099	2	15.637	2	38.792	4
t2.10	KKI - kaersutite megacryst	0.702856	7	0.512927	6	19.310	5	15.578	4	38.674	9
t2.11	KKI - kaersutite megacryst	0.702853	7			19.327	14	15.574	11	38.660	28
t2.12											
	<i>Otago: Alpine Dike and Outlier</i>										
t2.14	OU42071	0.703323	7	0.512936	8	19.675	5	15.651	4	38.810	10
t2.15	OU42071			0.512925	7	19.662	2	15.643	2	38.795	5
t2.16	Wilkin5B	0.703326	8	0.512883	5	20.030	1	15.660	0	39.611	1
t2.17											
	<i>Otago: Waipiata</i>										
t2.19	LSI4*	0.702988	5	0.512870	3	20.146	1	15.632	1	39.880	2
t2.20	OU54926	0.703261	7	0.512887	7	19.253	2	15.618	1	38.935	3
t2.21	OU54926	0.703273	6			19.252	2	15.615	2	38.926	4
t2.22	OU54935	0.702931	7	0.512853	5	20.449	1	15.653	1	40.120	3
t2.23	OU54935	0.702927	8			20.450	2	15.646	1	40.103	4
t2.24	LSII	0.702895	8	0.512858	9	20.346	5	15.642	4	40.082	9
t2.25	LSII					20.349	3	15.644	3	40.101	7
t2.26	OU66573*	0.702865	4	0.512916	3	19.970	0	15.647	0	39.442	1
t2.27											
	<i>Otago: Dunedin Volcano</i>										
t2.29	LSI22	0.703032	6	0.512871	8	20.189	3	15.664	2	39.802	5
t2.30	LSI23*	0.703088	5	0.512879	2	19.764	1	15.639	1	39.368	2
t2.31	OU22855	0.702834	5	0.512913	5	20.074	1	15.658	1	39.598	3
t2.32											
	<i>Canterbury: Timaru</i>										
t2.34	OU33298	0.703564	8	0.512857	7	18.952	1	15.612	1	38.799	2
t2.35	OU33298	0.703575	8			18.949	1	15.608	1	38.786	2
t2.36	OU33278	0.703745	6	0.512829	5	18.923	1	15.619	0	38.791	1
t2.37	OU33278					18.928	2	15.619	2	38.789	5
t2.38											
	<i>Campbell Plateau: Auckland Island</i>										
t2.40	OU 19560	0.703724	7	0.512832	8	18.850	1	15.619	1	39.007	3
t2.41	OU 19560	0.703720	8	0.512829	8	18.852	2	15.620	1	39.007	3
t2.42	OU 19560	0.703715	5			18.850	1	15.618	1	39.005	2
t2.43	OU 19560	0.703723	7								
t2.44	OU 19577*	0.703066	3	0.512897	3	19.376	2	15.621	2	39.237	5
t2.45	OU 19606	0.702933	5	0.512935	5	19.642	2	15.596	2	39.161	4
t2.46	OU 19606	0.702946	7			19.641	2	15.595	1	39.159	3
t2.47	OU 19564*	0.703458	2	0.512859	3	18.894	2	15.607	2	39.033	5
t2.48											
	<i>Campbell Plateau: Campbell Island</i>										
t2.50	OU36173	0.703415	7	0.512891	12	19.326	1	15.604	1	39.198	1
t2.51	OU36173	0.703433	7			19.320	2	15.597	1	39.172	4
t2.52	OU36174*	0.704995	2	0.512793	3	19.070	1	15.625	1	39.114	1
t2.53	OU36176*	0.703195	2	0.512910	3	19.517	3	15.602	2	39.268	5
t2.54	OU36163*	0.704019	2	0.512856	3	19.183	1	15.605	1	39.134	3

t2.55 Errors are  $2\sigma$  within run given to the least significant digit.

t2.56 \* Sr–Nd measured on TRITON TIMS, all others MAT262. For analytical details see Appendix 3.

88 separation of New Zealand from West Antarctica ceased  
 89 in the mid-Cretaceous, but Weaver and Smith [2]  
 90 proposed that Cenozoic intraplate volcanism was at

least in part related to shallow upwellings related to 91  
 local rifting events. In contrast, based on an apparent 92  
 crude WNW-ESE age progression of volcanism, Adams 93

94 [6] and Farrar and Dixon [7] proposed that intraplate  
 95 volcanism resulted from Zealandia over-riding a former  
 96 spreading center, manifested as a NNE-trending line of  
 97 asthenospheric upwelling. Coombs et al. [8] noted the  
 98 similarity in Sr and Nd isotopic composition of Cenozoic  
 99 basalts on the South Island of New Zealand to basalts  
 100 from Australia and Marie Byrd Land, Antarctica. These  
 101 three continental blocks were contiguous prior to 100 Ma  
 102 but rifted apart at c. 84 Ma, suggesting that the Cenozoic  
 103 volcanism resulted from melting of common, and  
 104 therefore lithospheric, source materials (e.g. [8–10]).  
 105 Lithospheric sources have been proposed for the  
 106 nephelinitic to tholeiitic volcanism in the South Auckland

107 volcanic field [11] and on the Chatham, Campbell and  
 108 Antipodes Islands [12]. In contrast, Finn et al. [4] included  
 109 the Cenozoic intraplate volcanism on New Zealand within  
 110 a “Diffuse Alkaline Magmatic Province”, encompassing  
 111 the easternmost part of the Indo-Australian Plate, West  
 112 Antarctica and the southwest portion of the Pacific Plate,  
 113 and attributed this magmatism to interaction between the  
 114 uppermost asthenospheric mantle and subduction-modified  
 115 subcontinental lithosphere.

116 In order to better understand the origin of Cenozoic  
 117 intraplate volcanism on New Zealand, we have acquired  
 118 new age ( $^{40}\text{Ar}/^{39}\text{Ar}$ ) and geochemical (major element,  
 119 trace element and Sr–Nd–Pb isotopic) data to assess  
 120

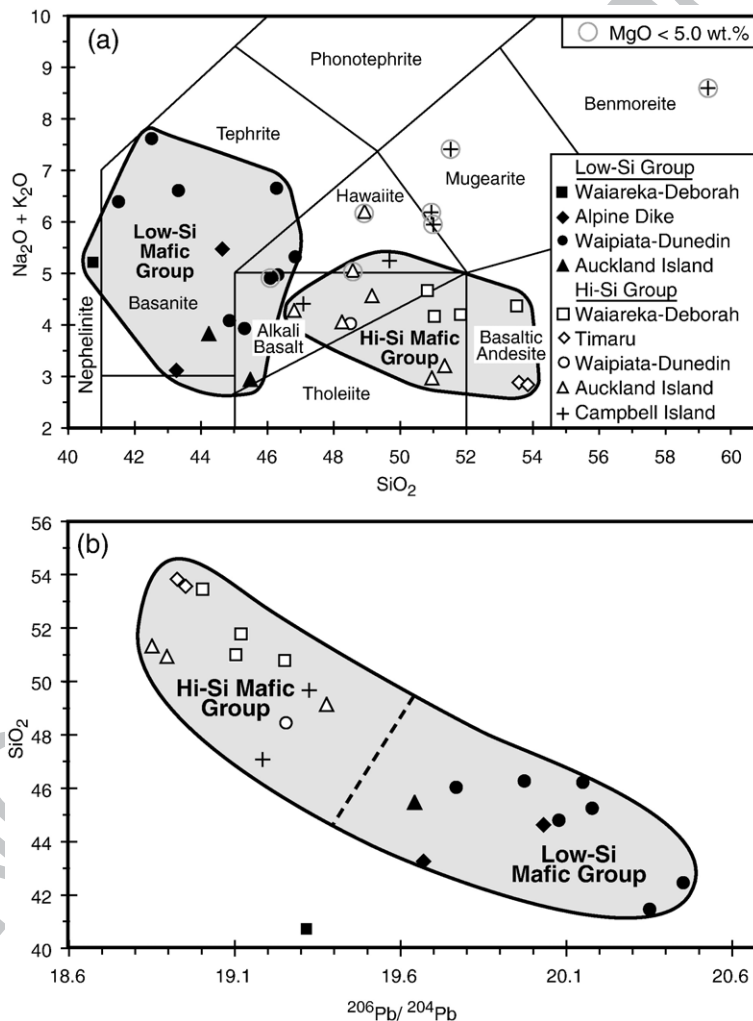


Fig. 2. a)  $\text{SiO}_2$  versus alkali ( $\text{Na}_2\text{O} + \text{K}_2\text{O}$ ) diagram after [22] for identification of rock types from the South Island of New Zealand and Campbell Plateau. Samples are divided into hi-Si ( $\text{SiO}_2 > 46$  wt.%; open symbols and +) and low-Si ( $\text{SiO}_2 < 46$  wt.%; filled symbols) groups. Symbols for low MgO (<5 wt.%) samples are circled. b)  $^{206}\text{Pb}/^{204}\text{Pb}$  versus  $\text{SiO}_2$  for mafic ( $\text{MgO} > 5$  wt.%) Zealandia intraplate volcanic rocks forms a negative correlation ( $y = -6.5908x + 176.71$ ) with  $R^2 = 0.83$ , excluding the Kakanui Mineral Breccia sample (for which major element data for whole rock sample OU53628 was combined with isotope data from kaersutite megacryst KK1). See Supplementary file 4 for geochemical data in this diagram.

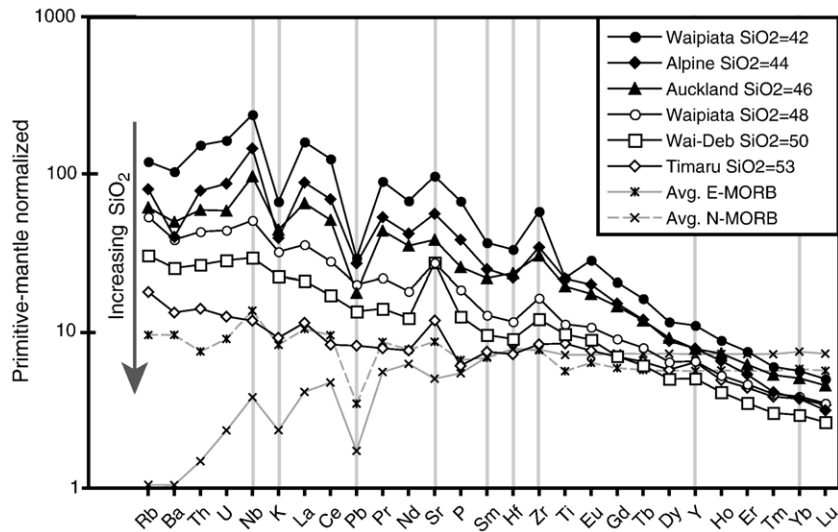


Fig. 3. Multi-element diagram for representative mafic ( $\text{MgO}=8\pm 2$  wt.%) samples from the South Island of New Zealand and the Campbell Plateau. Note the inverse correlation in mafic samples between  $\text{SiO}_2$  content and concentrations in intermediate to highly incompatible elements. With increasing  $\text{SiO}_2$ , negative K and Pb anomalies disappear, positive Zr anomaly becomes less pronounced and positive Sr anomaly becomes more pronounced. Compared to mid-ocean-ridge basalt (MORB), the intermediate and highly incompatible elements are generally enriched, whereas the heavy rare earth elements (HREE) are depleted. These chemical differences are consistent with the Zealandia intraplate volcanic rocks (nephelinite/basanites through tholeiites) being formed through lower degrees of melting of more enriched source material and at greater depths in the presence of residual garnet than MORB. In contrast, MORB is formed at higher degrees of melting of more depleted source material within the spinel stability field. In addition to having HREE depletion, the Zealandia tholeiites are distinct from enriched (E) MORB in that they do not have positive Nb or negative Pb anomalies. These chemical differences to MORB can be explained by interaction of the Zealandia tholeiites with (or in some cases such as Timaru, possibly derivation from) subduction-modified continental lithospheric mantle  $\pm$  continental crust. Samples in order of decreasing Nb are Waipiata OU54935, Alpine Dike Wilkin 5B, Auckland Islands R7517, Waipiata OU54926, Waiareka–Deborah OU55008 and Timaru OU33278. Average normal (N) and E MORB from [72]. Grey lines underlying the data for certain elements emphasize major incompatible element variations that correlate with variations in Si-saturation of the magmas. See Supplementary File 4 for geochemical data in this diagram.

120 possible age progressions in volcanism and the sources  
 121 of magma for volcanic rocks from Otago on the South  
 122 Island of New Zealand and from the Auckland and  
 123 Campbell Islands on the Campbell Plateau.

## 124 2. Results

### 125 2.1. Age determinations

126 Twenty-six intraplate volcanic samples from the South  
 127 Island of New Zealand and the Auckland and Campbell  
 128 Islands on the Campbell Plateau (see Supplementary File  
 129 1 for sample descriptions and locations) have been dated  
 130 with the  $^{40}\text{Ar}/^{39}\text{Ar}$  method (age data are summarized in  
 131 Table 1; analytical methods, detailed age data and age  
 132 diagrams are presented in Supplementary File 2).

133 Six samples from the Waiareka–Deborah Formation  
 134 [8] near Oamaru northeast of Dunedin (Fig. 1 inset)  
 135 have ages ranging from 34–40 Ma. Five Waiareka–  
 136 Deborah samples yielded the same age within error (all  
 137 errors in this paper are reported at the  $2\sigma$  confidence  
 138 level):  $34.2\pm 0.4$  Ma and  $34.3\pm 0.9$  Ma from glass from

the margin of the same tholeiitic pillow lava at 139  
 Boatmans Harbour,  $34.0\pm 0.6$  Ma from transitional 140  
 tholeiite,  $33.6\pm 1.8$  Ma from tholeiite,  $34.3\pm 0.5$  Ma 141  
 from tuff at Bridge Point and  $34.1\pm 0.1$  (single fusions) 142  
 and  $33.7\pm 0.3$  Ma (step heating analyses) from kaersu- 143  
 tite megacryst KK1 from the nephelinitic Kakanui 144  
 Mineral Breccia. Dasch et al. [13] determined a slightly 145  
 younger K–Ar age of  $31.6\pm 1.2$  Ma for the Kakanui 146  
 Mineral Breccia. The new age is consistent with the 147  
 Kakanui Mineral Breccia being located stratigraphically 148  
 in the uppermost Eocene, just beneath the Oligocene 149  
 boundary. The age of  $39.5\pm 1.8$  Ma is from a basaltic 150  
 andesite dike fragment (with chilled glassy margins) 151  
 within the tuff sequence at Bridge Point, indicating the 152  
 presence of older volcanism in the Oamaru area that 153  
 may not be exposed at the surface. 154

155 Seven alkali basalt to basanite samples from mono-  
 156 genetic volcanoes in the Waipiata volcanic field [8] yielded  
 157 ages of 11–25 Ma ( $11.1\pm 0.6$ ;  $14.1\pm 0.6$ ,  $14.4\pm 0.2$  and  
 158  $14.4\pm 0.2$  Ma (replicate analyses),  $17.1\pm 0.5$  and  $17.0\pm 0.5$   
 159 (replicate),  $21.4\pm 0.4$ ,  $22.0\pm 0.3$  and  $24.8\pm 0.6$  Ma),  
 160 considerably expanding the published K/Ar age range

161 of c. 13–16 Ma based on two age dates [14]. A single  
 162 basanitic sample from Nevis Bluff, regarded as a southern  
 163 outlier of the Alpine–Northwest Otago lamprophyric dike  
 164 swarm, produced an age of  $20.7 \pm 0.4$ , within the Waipiata  
 165 age range and at the young end of the Alpine–Northwest  
 166 Otago Dike Swarm range of ages, for which 15 K/Ar  
 167 whole rock and kaersutite ages (from 12 rock samples)  
 168 cluster between 23–32 Ma [15]. Cooper et al. [16] reported  
 169 Rb/Sr and U/Pb ages for four bodies in the same swarm  
 170 ranging from 20–25 Ma.

171 Five samples from the Dunedin Volcano (ranging from  
 172 alkali basalt and basanite to phonolitic and syenite)  
 173 produced ages of  $11.7 \pm 0.1$  Ma,  $13.0 \pm 0.2$  Ma,  $13.2 \pm$   
 174  $0.5$  Ma (single fusion) and  $13.0 \pm 0.6$  Ma (step heating  
 175 analyses) from the same sample,  $14.6 \pm 0.4$  Ma and  $16.0 \pm$   
 176  $0.4$  Ma, extending the previously determined K/Ar age  
 177 range of the Dunedin Volcano of 10–13 Ma [14] by c.  
 178 3 million years. The two oldest ages were obtained from

the Otago Peninsula for which no age data has been  
 previously published. The Dunedin Volcano appears to  
 have formed during the later part of the Waipiata volcanic  
 cycle near the center of the half-circular Waipiata field as  
 it is exposed on land; Waipiata volcanism also occurred  
 offshore. The age for a quartz tholeiite sample from  
 Timaru of  $2.6 \pm 0.4$  Ma agrees well with the K/Ar age of  
 $2.5 \pm 0.7$  Ma [17].

The  $^{40}\text{Ar}/^{39}\text{Ar}$  ages for three samples collected by  
 Wright [18,19] from the upper part of the northern or Ross  
 Volcano in the Auckland Islands are  $15.2 \pm 0.3$  Ma,  $16.7$   
 $\pm 0.1$  Ma and  $16.7 \pm 1.2$  Ma. Our ages overlap two ages of  
 14 and 16 Ma reported by Adams [20] from similar  
 localities, Ewing Island and Williamson Point. The  
 overall range of Adams' K/Ar ages for the deeply eroded  
 and complex Ross Volcano is 12–25 Ma. Available K/Ar  
 dates for the southern or Carnley Volcano, 19–37 Ma, are  
 from the Carnley Harbour area within the core of the

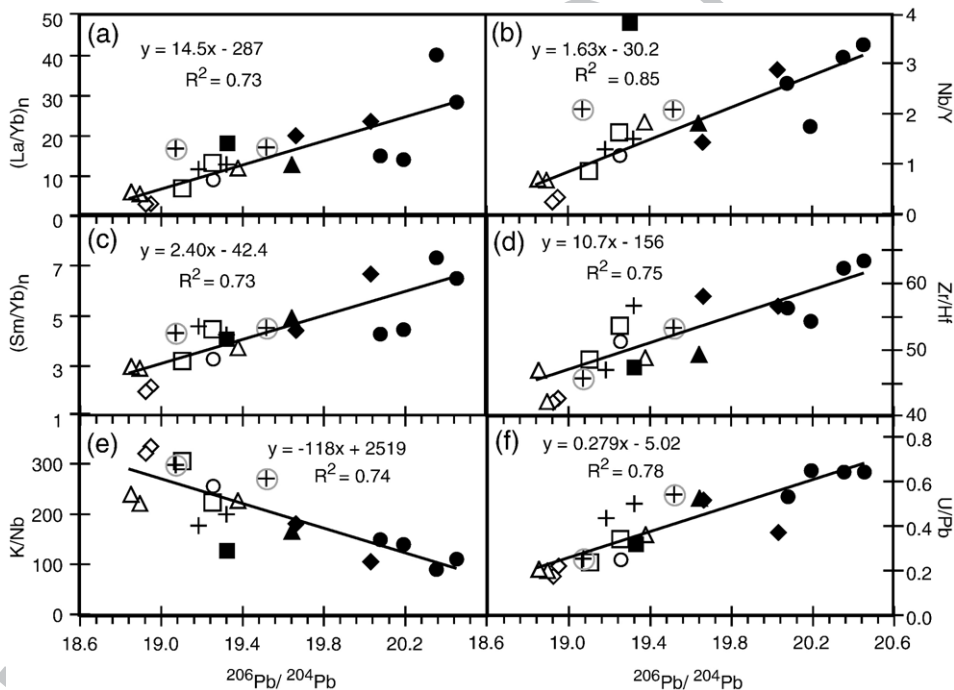


Fig. 4.  $^{206}\text{Pb}/^{204}\text{Pb}$  versus a)  $(\text{La}/\text{Yb})_n$  ( $n$  = normalized to primitive mantle after [73]), b) Nb/Y, c)  $(\text{Sm}/\text{Yb})_n$ , d) Zr/Hf and f) U/Pb correlate ( $R^2 = 0.73$ – $0.85$ ) positively, whereas  $^{206}\text{Pb}/^{204}\text{Pb}$  versus e) K/Nb correlates ( $R^2 = 0.74$ ) negatively. Positive correlation of Pb isotope ratios with  $(\text{La}/\text{Yb})_n$  and Nb/Y is consistent with low-Si rocks being derived from more enriched sources through lower degrees of melting than hi-Si rocks.  $(\text{Sm}/\text{Yb})_n$  in the low-Si rocks indicates residual garnet in the sources of all the Zealandia intraplate volcanic rocks but more residual garnet in the low-Si than hi-Si rocks. High Zr/Hf in all the rocks is consistent with eclogite (with modal clinopyroxene/garnet  $\geq 70\%$ ), whereas lower Zr/Hf in the more silicic rocks suggests greater degrees of eclogite melting up to  $\sim 50\%$  [53]. The high U/Pb and  $^{206}\text{Pb}/^{204}\text{Pb}$  ratios in the low-Si rocks indicate derivation from a source with high time-integrated  $^{238}\text{U}/^{204}\text{Pb}$  ( $\mu$ ) or a HIMU mantle source. The high K/Nb (and low U/Pb) in the hi-Si rocks are consistent with interaction of asthenospheric melts from HIMU sources with enriched mantle (EM) melts from the overlying subduction-modified (lithospheric) mantle and/or continental crust. Best-fit linear correlations calculated for mafic volcanics with  $\text{MgO} > 5$ , excluding the Kakanui Mineral Breccia. Kakanui Mineral Breccia incompatible element data are from matrix separate from sample OU53628 and the isotope data are from kaersutite megacryst KK1 in the Kakanui Mineral Breccia. Symbols are the same as in Fig. 2. See Table 2 and Supplementary File 4 for geochemical data in this diagram.

197 volcano [20], and probably do not represent the younger,  
 198 upper members of this shield volcano. Additional age  
 199 dating is necessary to confirm the long history of  
 200 volcanism on these islands.

201 The four Campbell Island ages ( $6.94 \pm 0.05$  Ma,  $6.6 \pm$   
 202  $0.6$  Ma and  $7.3 \pm 0.3$  Ma from feldspar and matrix step  
 203 heating analyses of the same sample and  $7.5 \pm 0.3$  Ma) fall

within the age range determined by the K/Ar method,  
 6.5–8.5 Ma, together with a discrepant date of 11.1 Ma for  
 a sample with low radiogenic argon and an imprecise  
 16 Ma age for an alkali gabbro [21]. The alkali gabbro  
 intrudes a unit consisting of marine sediments of mid- to  
 late Miocene age interbedded with and overlain by tuffs,  
 volcanic breccias and lignite. There is a rapid conformable

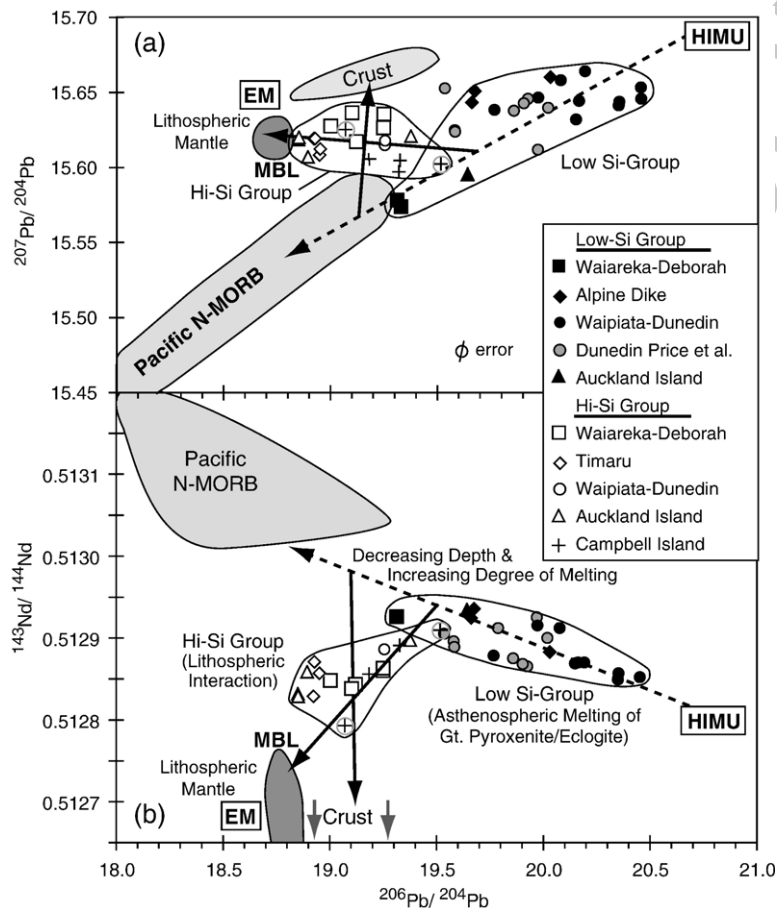


Fig. 5. On  $^{206}\text{Pb}/^{204}\text{Pb}$  versus a)  $^{207}\text{Pb}/^{204}\text{Pb}$  and b)  $^{143}\text{Nd}/^{144}\text{Nd}$  isotope correlation diagrams, the low-Si and hi-Si groups form nearly completely distinct fields, which require mixing of at least three components. The low-Si group rocks have more radiogenic Pb and less radiogenic Nd isotope ratios than normal mid-ocean-ridge basalt (N-MORB) and form an array between Pacific N-MORB and high  $\mu$  (HIMU)-type mantle, consistent with melting of garnet pyroxenite/eclogite within upwelling asthenosphere at greater depths and lower degrees of melting than N-MORB. The dashed arrow through the low-Si group array indicates increasing degrees of melting of the pyroxenite/eclogite component with decreasing depth of melting. N-MORB is formed by the highest degrees of melting, primarily in the spinel stability field, with the largest contribution from the most depleted (peridotitic) source material. Hi-Si Zealandia rocks form a crude array extending from the low-Si group field towards enriched mantle (EM) or the field of c. 108 Ma Group B and C dikes from Marie Byrd Land (MBL) Antarctica [27]. In contrast to the Group A dikes, which have HIMU-type geochemical characteristics and more radiogenic Pb and Nd isotope ratios, the Group B and C dikes (gray field labeled MBL) are characterized by 1) low  $\text{Fe}_2\text{O}_3^{\text{t}}$  (<13 wt.%) and  $\text{TiO}_2$  (<2.2 wt.%), 2) distinct Nb and Ta troughs and distinct peaks at fluid-mobile elements such as Rb, K and Sr on chondrite-normalized multi-element diagrams (subduction-type incompatible element signatures), and 3) the most radiogenic Sr and least radiogenic Nd and Pb isotope ratios. The Group B and C dikes are interpreted to most closely reflect the lithospheric mantle composition beneath Gondwana [27]. At least parts of the subduction-modified lithospheric mantle beneath Gondwana (Marie Byrd Land and Zealandia), however, is expected to have had more extreme EM-type compositions with less radiogenic Pb and Nd isotope compositions than the Group B and C dikes. Solid arrows indicate interaction of hi-Si melts (alkali basalts and tholeiites) derived through melting of upwelling asthenosphere with the Zealandia continental lithosphere (mantle and crust). Data from Dunedin volcano [74] is also shown. Field for representative New Zealand sediments is from Tappenden [26]. In (b) the errors are smaller than the symbols.



211 transition from volcanoclastic deposits to the overlying  
 212 lavas forming the island volcano. In conclusion, the  
 213 subaerial part of the Campbell Island volcano is likely to  
 214 have formed within 1–2 million years.

## 215 2.2. Geochemistry

216 New major element, trace element and Sr–Nd–Pb  
 217 isotope data and analytical methods are presented in  
 218 Table 2 and Supplementary Files 3 and 4. Supplemen-  
 219 tary File 4 contains all geochemical data in a single  
 220 spreadsheet. Samples range from tholeiite to basaltic  
 221 andesite (Timaru, Waiareka–Deborah, Auckland  
 222 Islands), alkali basalt to benmoreite (Dunedin Volcano,  
 223 Waipiata and Auckland and Campbell Islands) and  
 224 basanite/nephelinite (Waiareka–Deborah, Alpine Dike  
 225 Swarm, Auckland Islands, Waipiata and Dunedin Vol-  
 226 cano) based on the SiO<sub>2</sub> versus alkali diagram [TAS  
 227 after 22] (Fig. 2). Mafic (MgO > 5 wt.%) samples are  
 228 divided into hi-Si (SiO<sub>2</sub> > 46 wt.%) and low-Si  
 229 (SiO<sub>2</sub> < 46 wt.%) groups. Auckland Island samples  
 230 extend to more evolved hawaiitic compositions and  
 231 Campbell Island samples range from alkali basalt to  
 232 benmoreite. Basaltic andesites can be derived from  
 233 tholeiites through removal of olivine, clinopyroxene,  
 234 plagioclase and minor Fe–Ti oxides, whereas benmor-  
 235 eites can be derived from alkali basalts primarily through  
 236 removal of these phases plus apatite.

237 In the mafic samples, SiO<sub>2</sub> is negatively correlated  
 238 with FeO<sup>t</sup> (total iron as FeO) and CaO and incompatible  
 239 element abundances (e.g. Rb, Ba, Th, U, Nb, Ta, K,  
 240 LREE, Sr, P and Ti, excluding Nevis Bluff sample for Sr  
 241 and Ba). On multi-element diagrams (e.g. Fig. 3), the  
 242 samples display enrichment in highly to moderately  
 243 incompatible elements with all samples having steep  
 244 heavy rare earth element (HREE) patterns and (Sm/Yb)<sub>n</sub>  
 245 (n = normalized to primitive mantle), (Dy/Yb)<sub>n</sub> and (Zr/  
 246 Y)<sub>n</sub> > 1. With increasing SiO<sub>2</sub>-saturation in the mafic  
 247 rocks (basanite to tholeiite), the Nb and Zr peaks and the  
 248 K and Pb troughs become less pronounced, whereas the  
 249 Sr peak becomes more accentuated. These variations are  
 250 reflected in negative correlations of SiO<sub>2</sub> with ratios of  
 251 more to less incompatible elements (e.g. La/Yb, La/Sm,  
 252 Nb/Y, Th/Yb, Zr/Y and U/Pb) and with ratios of  
 253 elements with similar bulk partition coefficients during  
 254 mantle melting (e.g. Zr/Hf, Nd/Pb and Ce/Pb). SiO<sub>2</sub>,  
 255 however, correlates positively with ratios of fluid-  
 256 mobile to less fluid-mobile elements (e.g. (K, Rb, Ba,  
 257 Sr, Pb)/Nb and Pb/(U, Nd, Ce)). Excluding evolved  
 258 (benmoreite and mugearite) samples, <sup>206</sup>Pb/<sup>204</sup>Pb iso-  
 259 tope ratios form inverse correlations with SiO<sub>2</sub> (Fig. 2b)  
 260 and (Ba, Rb, K, Pb, Sr)/Nb ratios and positive corre-

261 lations with FeO<sup>t</sup>, CaO, most incompatible element  
 262 concentrations and La/Yb, La/Sm, Nb/Y, Th/Yb, Zr/Hf  
 263 and (Ce, Nd, U, Th)/Pb ratios (e.g. Fig. 4). On isotope  
 264 correlation diagrams (<sup>87</sup>Sr/<sup>86</sup>Sr versus <sup>143</sup>Nd/<sup>144</sup>Nd and  
 265 <sup>206</sup>Pb/<sup>204</sup>Pb versus <sup>207</sup>Pb/<sup>204</sup>Pb, <sup>208</sup>Pb/<sup>204</sup>Pb and  
 266 <sup>143</sup>Nd/<sup>144</sup>Nd), the more SiO<sub>2</sub>-saturated (hi-Si) mafic  
 267 rocks form fields distinct from those of highly SiO<sub>2</sub>-  
 268 undersaturated (low-Si) rocks, with the low-Si rocks  
 269 having compositions similar to high time-integrated  
 270 <sup>238</sup>U/<sup>204</sup>Pb (μ) (or HIMU) ocean island basalts (OIBs)  
 271 and the hi-Si rocks having compositions tending  
 272 towards the enriched mantle (EM) components observed  
 273 in OIB (e.g. Fig. 5).

## 274 3. Discussion

### 275 3.1. Temporal and spatial variations of Cenozoic 276 intraplate volcanism

277 Late Cretaceous and Cenozoic tholeiitic to nephelin-  
 278 itic intraplate volcanism has been commonplace and  
 279 widespread in New Zealand and on the Chatham Rise  
 280 and the Campbell Plateau [2]. The Late Cretaceous  
 281 intraplate volcanism (~100–65 Ma) forming the  
 282 Mandamus Igneous Complex (e.g. [23]), the Tapuae-  
 283 nuku Igneous Complex [24], the Hohonu Range [16]  
 284 and the Southern Volcanics of the Chatham Islands  
 285 [12,25] is probably associated with the final phase of  
 286 Gondwana breakup in which the micro-continent  
 287 Zealandia separated from West Antarctica and may in  
 288 part reflect the involvement of a mantle plume head in  
 289 this breakup [2,12,24,26,27].

290 Cenozoic intraplate volcanism on Zealandia began  
 291 with Paleocene volcanism offshore of Otago (Fig. 1  
 292 inset; 1 km of tuffs in the Endeavour 1 Drillhole [8]), in  
 293 South Westland (Arnott basalt [28,29]) and possibly in  
 294 Marlborough (basanitic dikes in the Tapuaenuku  
 295 Igneous Complex; [24]). The Arnott basalt, outcropping  
 296 west of the Alpine Fault (on the Australian Plate), was  
 297 located northwest of the Auckland Islands at the time of  
 298 its formation, ~500 km south of its present location  
 299 [16,30,31]. Paleocene to Lower Eocene tholeiitic basalts  
 300 are also present in Canterbury [32] (e.g. the View Hill  
 301 Volcanics near Oxford have been dated at 51.7 ± 2.4 Ma  
 302 and 47.9 ± 3.6 Ma [33]). In the Late Eocene (~34–  
 303 41 Ma), nephelinitic to tholeiitic volcanic rocks were  
 304 erupted in eastern Otago (Waiareka–Deborah Volcanics;  
 305 Table 1) and on the Chatham Islands (Northern  
 306 Volcanics; [25,34]). Our new results show that nephe-  
 307 linitic through tholeiitic rocks were erupted simulta-  
 308 neously within error of 34.1 Ma in a very restricted area  
 309 in Otago near Oamaru. The Lower Oligocene Otitia

310 Basalt outcrops in South Westland [35]. Relatively large  
 311 volumes ( $\sim 100 \text{ km}^3$ ) of Early Oligocene ( $\sim 34\text{--}28 \text{ Ma}$ )  
 312 tholeiitic to nephelinitic volcanic rocks are widespread  
 313 in northern Canterbury and eastern Marlborough (e.g.  
 314 Cookson [36] and Oxford [37] volcanic rocks). Some of  
 315 the lamprophyric Alpine Dikes, ranging from nephelin-  
 316 ite, basanite and carbonatite to phonolite and trachyte  
 317 [38], intruded in the Oligocene and the Early Miocene  
 318 (Table 1 and [15,16]).

319 Neogene and Quaternary intraplate volcanism was  
 320 widespread on Zealandia. Our new data show that dozens  
 321 of alkali basaltic and basanitic to mugearitic and phonolitic  
 322 monogenetic centers formed in eastern Otago as part of the  
 323 Waipiata volcanic field [8] during the Late Oligocene to  
 324 Late Miocene (25–11 Ma; Table 1), overlapping onto the  
 325 older (40–34 Ma) Waiareka–Deborah volcanic field from  
 326 the south (Fig. 1b). The mid-Miocene (c. 16–10 Ma; Table  
 327 1 and [14]) Dunedin composite shield volcano, which lies  
 328 geographically within the diffuse Waipiata volcanic field,  
 329 has compositions ranging from alkali basalt and basanite to  
 330 trachyte and phonolite, strongly overlapping the compo-  
 331 sitional range of the Waipiata volcanics. The Dunedin  
 332 Volcano also temporally overlaps both the Waipiata  
 333 volcanism and volcanism on the Auckland Islands as  
 334 reported here (17–15 Ma; Table 1; [20,39]). The large  
 335 composite Lyttelton ( $350 \text{ km}^3$ ) and Akaroa ( $1200 \text{ km}^3$ )  
 336 shield volcanoes on Banks Peninsula formed between 12–  
 337 6 Ma. With decreasing age, volcanism on Banks Peninsula  
 338 produced first andesites through rhyolites, then tholeiites  
 339 and alkali basalts through trachytes, and finally tholeiites  
 340 through nephelinites [3,40]. The Banks Peninsula volca-  
 341 nism overlaps in age with alkali basaltic to benmoreitic  
 342 volcanism on Campbell Island as reported here (6.6–  
 343 7.5 Ma; Table 1, Fig. 1) and widespread basanitic through  
 344 tholeiitic (and their differentiates) volcanism on the  
 345 northwestern part of the North Island, which contains the  
 346 Northland (9.7 Ma to Recent) and Auckland (2.7 Ma to  
 347 Recent) Volcanic Provinces [11]. Pliocene volcanism also  
 348 took place on Chatham Island (basanitic to phonolite; 6–  
 349 3 Ma [12,25], and near Geraldine and Timaru in Canter-  
 350 bury on the South Island (tholeiitic; 2.6 Ma; Table 1 and  
 351 [17]). Pleistocene ( $\leq 1 \text{ Ma}$  [41]) volcanic rocks (basanitic  
 352 to phonolitic) are present on the Antipodes Island [34] at  
 353 the northeastern edge of the Campbell Plateau.

354 In summary, it has long been recognized that Cenozoic  
 355 intraplate volcanism on Zealandia, a region of relatively  
 356 mature continental crust, was nearly continuous and widely  
 357 dispersed [2]. The new age results from Otago presented  
 358 here show that 1) compositionally diverse nephelinitic to  
 359 tholeiitic volcanic rocks of the Waiareka–Deborah For-  
 360 mation were erupted simultaneously (within analytical  
 361 errors), 2) the alkaline Waipiata field of monogenetic

362 centers formed over  $\geq 14$  million years (c. 25–11 Ma) 362  
 363 expanding the published age range (13–16 Ma; [14]) by 363  
 364 11 Ma, 3) volcanism associated with the Dunedin Volcano 364  
 365 (16–<12 Ma) began 3 million years earlier than previously 365  
 366 reported, and 4) the Dunedin volcano formed within the 366  
 367 Waipiata field during the final stages of Waipiata 367  
 368 volcanism. These results provide important constraints 368  
 369 on the timing and ultimately origin of different types of 369  
 370 intraplate volcanism on Zealandia. 370

### 371 3.2. Problems with previously proposed models for the 371 372 origin of intraplate volcanism 372

373 Diffuse intraplate volcanism in Zealandia had a wide 373  
 374 compositional range including tholeiite through rhyolite, 374  
 375 alkali basalt through trachyte and basanite through 375  
 376 phonolite (and syenite) with rarer nephelinite and 376  
 377 carbonatite. No systematic age progressions (except on 377  
 378 small scales of  $<100 \text{ km}$ , e.g. Banks Peninsula) are 378  
 379 obvious in the distribution of the volcanic rocks. Multiple 379  
 380 episodes of volcanism occurred 1) at the same location 380  
 381 (e.g. Chatham Island; Late Cretaceous, Eocene and 381  
 382 Pliocene [12,25] or within restricted areas (e.g. Waiar- 382  
 383 eka–Deborah, Waipiata and Dunedin Volcanism occurred 383  
 384 within an area of  $\sim 100 \text{ km}$  across from c. 40–10 Ma), and 384  
 385 2) at widely differing locations at the same time (e.g. 385  
 386 Auckland Island, Dunedin Volcano and Waipiata volca- 386  
 387 nics; Banks Peninsula, Campbell Island and Northland 387  
 388 Volcanic Province). Zealandia drifted  $\sim 4000 \text{ km}$  during 388  
 389 the Cenozoic ( $\sim 6.1 \text{ cm/yr}$  on average to the NW [42,43] 389  
 390 and  $\sim 1800 \text{ km}$  between 40 and 10 Ma during which time 390  
 391 the Waiareka–Deborah, Waipiata and Dunedin magmas 391  
 392 erupted in a restricted area of  $\sim 100 \text{ km}$  across. Therefore 392  
 393 the Cenozoic intraplate volcanism is incompatible with 393  
 394 the hotspot (mantle plume) hypothesis, which predicts 394  
 395 chains of volcanoes that become progressively older in the 395  
 396 direction of plate motion, unless we invoke a swarm of 396  
 397 weak pulsating plumes. No obvious plume-like structures, 397  
 398 however, have been identified in seismic tomographic 398  
 399 images beneath Zealandia [4]. Spatially restricted volca- 399  
 400 nism occurring over long time periods is also inconsistent 400  
 401 with the passage of Zealandia over a linear, NE-oriented 401  
 402 region of upper mantle upwelling [6,7]. Major continental 402  
 403 rifting ended in the mid-Cretaceous, and later extension is 403  
 404 spatially coincident with only a minority of Cenozoic 404  
 405 intraplate volcanic events, so continental rifting accom- 405  
 406 panied by major lithospheric thinning also fails to explain 406  
 407 the origin of the widespread Cenozoic intraplate volca- 407  
 408 nism of Zealandia. Furthermore, it is unlikely that 408  
 409 Cenozoic extension caused enough lithospheric thinning 409  
 410 to generate the larger degrees and extents of melting 410  
 411 required, for example, to form tholeiitic melts and large 411

412 composite volcanoes, such as the Dunedin (possibly  
413 800 km<sup>3</sup> if possible intrusives are included [44]), Banks  
414 Peninsula (~1600 km<sup>3</sup>), Auckland Island or Campbell  
415 Island volcanoes. It is also difficult to conceive of  
416 mechanisms for causing such relatively short ( $\leq 6$  m.y.)  
417 but extensive melting events solely in the lithosphere  
418 through the melting of metasomatized lithosphere via heat  
419 conduction from the asthenosphere, since conductive  
420 heating is an inefficient process for producing large  
421 volumes of melt [45]. Finally, although 30% assimilation  
422 of continental crust by a basanitic melt could explain  
423 much of the major element chemistry of the tholeiites, the  
424 lower abundances of most incompatible elements in the  
425 tholeiites compared to basanites and common crustal  
426 rocks in New Zealand are inconsistent with such a model.

### 427 3.3. Generation and sources of Cenozoic intraplate 428 volcanism

429 Systematic differences that correlate with degree of  
430 SiO<sub>2</sub>-saturation of the parental melts exist in the major  
431 element, trace element and Sr–Nd–Pb isotopic composi-  
432 tions of the Cenozoic Zealandia intraplate volcanic rocks.  
433 As noted above, the mafic (MgO > 5 wt.%) intraplate  
434 volcanic rocks can be divided into two groups based on  
435 their SiO<sub>2</sub> contents: 1) low-Si group with SiO<sub>2</sub> < 46%  
436 consisting primarily of basanites but also alkali basalt,  
437 nephelinite and tephrites, and 2) hi-Si group with  
438 SiO<sub>2</sub> > 46 wt.% consisting of alkali basalt through  
439 hawaiite and tholeiite through basaltic andesite. In  
440 contrast to the hi-Si group, the low-Si group has 1) high  
441 FeO<sup>t</sup> and CaO, 2) high incompatible element abundances  
442 (e.g. Rb, Ba, Th, U, Nb, Ta, K, LREE, Sr, P and Ti), 3)  
443 high ratios of more to less incompatible elements (e.g. La/  
444 Yb, La/Sm, Nb/Y, Th/Yb, Zr/Y, U/Pb, including HREE  
445 ratios such as Sm/Yb, Dy/Yb and Tb/Yb), 4) high ratios of  
446 elements with similar bulk partition coefficients during  
447 melting of mantle rocks (e.g. Zr/Hf, Nd/Pb and Ce/Pb),  
448 and 5) low ratios of fluid-mobile to less fluid-mobile  
449 elements (e.g. (K, Rb, Ba, Sr, Pb)/Nb and Pb/(U, Nd, Ce))  
450 (e.g. Figs. 3 and 4). Finally the low-Si group extends to  
451 less radiogenic Sr and more radiogenic Nd and Pb isotopic  
452 compositions than the hi-Si group and falls on a mixing  
453 array between the ocean island basalt HIMU and the  
454 Pacific MORB components (Fig. 5). The hi-Si group  
455 extends from the low-Si array towards enriched mantle  
456 (EM) and specifically towards mid-Cretaceous volcanic  
457 rocks from Marie Byrd Land Antarctica [27] (Fig. 5),  
458 which provide insights as to the composition of the  
459 lithospheric mantle beneath western Gondwana of which  
460 Zealandia was a part until c. 84 Ma. The wide range of  
461 geochemical differences between the low-Si and hi-Si

462 volcanic rocks indicates that the melts were formed under  
463 fundamentally different conditions, to be discussed below.

464 Comparison of the major element compositions of the  
465 Cenozoic intraplate Zealandia basalts with melts formed  
466 experimentally at high pressures can provide important  
467 insights about the source(s) of the basalts. Such high-  
468 pressure (1.5–7.0 GPa) experiments have been carried out  
469 on a wide array of possible mantle compositions including  
470 volatile-free peridotite (e.g. [46]), peridotite+CO<sub>2</sub> [47],  
471 peridotite–basalt mixtures [48], garnet pyroxenite [49,50]  
472 and eclogite+CO<sub>2</sub> [51]. Comparison of the melts formed  
473 at a given MgO (e.g. 10–12 wt.%) in the high-pressure  
474 melting experiments in the sequence eclogite+CO<sub>2</sub>,  
475 garnet pyroxenite, peridotite–basalt mixtures to volatile-  
476 free peridotite shows that there is a general increase in  
477 SiO<sub>2</sub> (from <40 to ~52 wt.%) and Al<sub>2</sub>O<sub>3</sub> and a general  
478 decrease in CaO, FeO<sup>t</sup> and TiO<sub>2</sub> in the melts (see  
479 compilation in [51], their Fig. 12). The mafic Zealandia  
480 intraplate rocks fall within the range defined by these  
481 experimental results. The major element contents and  
482 inverse correlations of SiO<sub>2</sub> with CaO, FeO<sup>t</sup> and TiO<sub>2</sub> in  
483 the Zealandia rocks suggest that the low-Si melts formed  
484 from sources containing carbonated eclogite, whereas the  
485 hi-Si melts formed through greater degrees of melting of a  
486 volatile-free peridotite±eclogite/pyroxenite source.

487 The negative correlations of SiO<sub>2</sub> with incompatible  
488 element abundances and ratios of more to less  
489 incompatible elements are consistent with derivation  
490 of more Si-rich melts through increasing degrees of  
491 partial melting of more depleted sources with decreasing  
492 depth (e.g. [46,52]). The steep HREE patterns (e.g. (Sm/  
493 Yb)<sub>n</sub> and (Dy/Yb)<sub>n</sub> > 1) indicate the presence of residual  
494 garnet in the source of all parental intraplate melts. The  
495 high (super chondritic) Zr/Hf ratios of all melts could  
496 result from melting of eclogite (or garnet pyroxenite)  
497 with high clinopyroxene/garnet modes of  $\geq 70$  in their  
498 source(s) [53,54]. Based on the calculations of Perter-  
499 mann et al. ([53]; see their Fig. 10), the range in Zr/Hf  
500 and Sm/Yb in the New Zealand rocks can reflect  
501 eclogite melt fractions of several percent for the  
502 basanites to about 50% for the tholeiites.

503 The trace element abundances of the New Zealand  
504 intraplate volcanic rocks (Fig. 3) are characteristic of  
505 ocean island basalts (OIBs). They are enriched compared  
506 to MORB and have different trace element characteristics  
507 (patterns on multi-element diagrams) than subduction  
508 zone basalts that display highly spiked patterns with  
509 relative enrichments in fluid-mobile elements (e.g. Rb,  
510 Ba, U, K, Pb and Sr) but relative depletion in fluid-  
511 immobile elements (e.g. Nb), resulting in high (Rb, Ba, U,  
512 K, Pb, Sr)/Nb and low (Ce, Nd, U)/Pb ratios. The trace  
513 element patterns of the low-Si rocks, characterized by

514 peaks at Nb and troughs at K and Pb, and their high Nd/  
515 Pb, Ce/Pb and U/Pb and radiogenic Pb isotope ratios  
516 indicate derivation from a HIMU-type mantle source.  
517 HIMU trace element and isotopic compositions are  
518 characteristic of volcanic rocks from ocean islands such  
519 as Mangaia, Tubuaii and St. Helena, interpreted to result  
520 from the presence of ancient (c. 1–2 Ga) recycled ocean  
521 crust in their sources (e.g. [55]). Although the low-Si  
522 Zealandia samples have elevated Pb isotope ratios (e.g.  
523  $^{206}\text{Pb}/^{204}\text{Pb}=19.3\text{--}20.5$ ), they are mostly not as high as  
524 those of the endmember HIMU-type ocean island  
525 localities mentioned above (with  $^{206}\text{Pb}/^{204}\text{Pb}$  of 20.5–  
526 22.0). On Sr–Nd–Pb isotope correlation diagrams, the  
527 low-Si rocks form an array between Pacific N-MORB and  
528 the HIMU endmember ocean islands. The less radiogenic  
529 Pb isotopic composition of the low-Si rocks from  
530 Zealandia compared to endmember HIMU could either  
531 reflect lower time-integrated parent/daughter (U/Pb and  
532 Th/Pb) ratios in the Zealandia sources for similar time  
533 periods, or similar (or higher) parent/daughter ratios in  
534 their sources for shorter periods of time. The similarity in  
535 U/Pb and Th/Pb ratios in the Zealandia intraplate  
536 volcanism and ocean island basalts, and location of  
537 much of the low-Si field to the right of the extended  
538 MORB basalt array on both Pb isotope diagrams, in  
539 particular on the thorogenic Pb isotope diagram (not  
540 shown), favor the latter possibility. Therefore, relatively  
541 young recycled ocean crust (eclogite) or young pyroxenite  
542 layers of igneous origin are likely to be present in the  
543 sources of the Zealandia intraplate volcanic rocks.

544 In accordance with the lack of evidence for mantle  
545 plumes beneath Zealandia and the problem of generating  
546 large volumes of entirely lithospheric melting (e.g. on the  
547 scale necessary to form a shield volcano), we favor  
548 generation of most of the Zealandia intraplate melts from  
549 asthenospheric sources. Finn et al. [4] have shown that the  
550 south Pacific asthenosphere has unusually low seismic  
551 velocities and propose that volcanism results from decom-  
552 pression melting of upwelling warm ( $\sim 1300\text{--}1400\text{ }^\circ\text{C}$ )  
553 Pacific mantle and partial melting of the base of the  
554 metasomatized subcontinental lithosphere. Compared to  
555 MORB, the intermediate and highly incompatible  
556 elements of all the Cenozoic intraplate volcanic rocks  
557 are generally enriched, whereas the heavy rare earth  
558 elements (HREE) are depleted. These chemical differ-  
559 ences are consistent with the Zealandia intraplate volcanic  
560 rocks being formed through lower degrees of melting  
561 from more enriched (eclogitic/pyroxenitic) source mate-  
562 rial and at greater depths in the presence of residual garnet,  
563 than MORB. In contrast, MORB is formed at higher  
564 degrees of melting of more depleted source material  
565 predominantly within the spinel stability field.

566 The isotope data for the low-Si group forms an array  
567 between the MORB and HIMU sources (Fig. 5), sug-  
568 gesting that the source of these rocks is the upper mantle,  
569 which contains some HIMU component. As discussed  
570 above, the HIMU component is likely to reflect younger  
571 eclogite/garnet pyroxenite than commonly sampled by  
572 mantle plumes. The MORB source upper mantle may  
573 contain 5% pyroxenitic/eclogitic layers in a peridotitic  
574 matrix [56]. Since altered oceanic crust contains a sig-  
575 nificant amount of calcium carbonate in vugs and veins, at  
576 least some of the eclogite in the mantle is likely to be  
577 carbonated. Carbonated eclogite could also be created by  
578 other processes within the mantle, for example crystalli-  
579 zation of carbonate-rich melts [57]. Dasgupta et al. [51]  
580 present a model for melting and metasomatism in up-  
581 welling carbonated oceanic mantle (containing carbonat-  
582 ed peridotite and eclogite or pyroxenite) that can explain  
583 the geochemistry of the Cenozoic Zealandia mafic vol-  
584 canic rocks. Carbonated low-silicate melts of eclogite/  
585 pyroxenite and peridotite, such as melilitites, nephelinites  
586 and basanites, will form in the deeper parts of the  
587 upwelling mantle column, whereas  $\text{CO}_2$  absent melting of  
588 eclogite/pyroxenite and peridotite will commence at  
589 higher levels in the upwelling column, producing high-  
590 silica alkali basalts and tholeiites. In contrast to the mid-  
591 ocean-ridge setting, the continental lithosphere (thicker  
592 than oceanic lithosphere) precludes extensive melting in  
593 the spinel stability field (Fig. 6) and therefore the  
594 Zealandia intraplate melts may be similar to melts from  
595 the deeper portions of the MORB melting column. Melts  
596 in equilibrium with garnet, however, are rarely preserved  
597 at mid-ocean ridges, due to the swamping effect of large  
598 volumes of melts formed at shallower depths. In con-  
599 clusion, because of its greater thickness, continental  
600 lithosphere may allow sampling of the lower portions of  
601 the MORB (upwelling upper mantle) melting column.  
602 Variations in the thickness of the continental lithosphere  
603 may ultimately control the type of melting and the style  
604 and composition of the ensuing volcanism. A fundamen-  
605 tal question, however, remains: What triggers the up-  
606 welling of upper mantle beneath Zealandia and what  
607 controls its location and duration? This will be discussed  
608 in the next section.

609 First we need to discuss some additional aspects of the  
610 geochemistry of the hi-Si rocks that are not consistent  
611 with asthenospheric melting. Although the trace element  
612 abundances of the hi-Si rocks are similar to those of  
613 ocean island alkali basalts and tholeiites, the almost  
614 smooth incompatible trace element patterns (except for  
615 positive Sr anomaly) without a pronounced Nb peak and  
616 Pb trough of the samples with the highest silica on the  
617 multi-element diagram (Fig. 3), as reflected for example

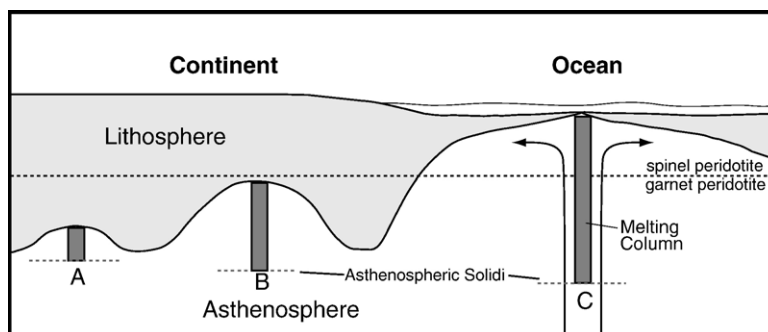


Fig. 6. Melting model illustrating the difference lengths of the Zealandia (A and B) and MORB (C) melting columns, i.e. depth intervals over which melting occurs, which extend from the asthenospheric solidus (based on temperature of the upwelling mantle) to the base of the lithosphere. The deeper the mantle that is sampled by the upwelling, the hotter the upwelling mantle will be and thus the solidus will be crossed at greater depth, resulting in greater overall degrees of melting. Beneath continental lithosphere, basanites and possibly nephelinites (melting column A) can be formed by low degrees of melting of garnet pyroxenite/eclogite within the shortest melting columns, resulting from the least amount of upwelling asthenosphere. Greater asthenospheric upwelling and melting of the garnet pyroxenite/eclogite component occur where greater amounts of continental lithosphere have been removed (melting column B), producing alkali basalts and tholeiites with garnet in the residuum. Melting column B is longer, since the hotter mantle from greater depth will cross the solidus earlier and melting will continue to shallower depths. The longest melting columns exist beneath mid-ocean ridges (C), where due to the thin oceanic lithosphere extensive melting takes place in the spinel peridotite stability field, forming MORB tholeiites.

618 by the high (Ba, K, Pb, Sr)/Nb and the low (Ce, Nd, U,  
619 Th)/Pb ratios, are not characteristic of either MORB or  
620 most OIB. The trace element characteristics of the hi-Si  
621 rocks, however, can be explained through higher degrees  
622 (than required to generate the low-Si rocks) of melting of  
623 a garnet peridotite+eclogite (or garnet pyroxenite)  
624 source and subsequent mixing with melts having  
625 incompatible element compositions similar to subduc-  
626 tion zone or crustal melts.

627 Several considerations favor a continental lithospheric  
628 source for the EM-type component. First, the more  
629 saturated melts are likely to have formed at shallower  
630 depths, as also proposed by Cook et al. [11] for the alkali  
631 basaltic and tholeiitic South Auckland volcanic rocks.  
632 Second, Zealandia was located at the edge of the  
633 Gondwana margin above a subducting slab for most of  
634 the Mesozoic. Hydrous subduction zone melts have the  
635 appropriate trace element and isotopic composition for the  
636 EM endmember and are likely to have overprinted  
637 (metasomatized) the Zealandia lithospheric mantle with  
638 this signature while it was still part of Gondwana [4,11].  
639 The trend of the hi-Si group towards the field for mid-  
640 Cretaceous Marie Byrd Land volcanic rocks, believed to  
641 have compositions most closely resembling those of the  
642 lithospheric mantle beneath Gondwana [27], further  
643 supports lithospheric interaction/derivation of the hi-Si  
644 melts. Melting of a hydrous Zealandia lithospheric mantle  
645 could have possibly even generated some of the olivine  
646 tholeiitic melts [58]. It has been shown that historic  
647 tholeiites in the Canary Islands – only present on the  
648 easternmost and thus presumably oldest island of  
649 Lanzarote – can be derived through mixing between

basanites (~50–60%) derived from sublithospheric 650  
sources and a high silica melt component (~40–50%), 651  
produced either by incongruent dissolution of orthopyr- 652  
roxene during direct reaction of basanitic melt with the 653  
lithosphere or by diffusive infiltration of alkalis (DIA) 654  
from the basanites into the surrounding lithosphere [59]. 655  
Similar processes can also explain the generation of some 656  
of the Zealandia tholeiitic melts, such as those erupted at 657  
Timaru and Geraldine, that produced similar amounts of 658  
tholeiite as the six year Timanfaya eruption on Lanzarote 659  
(2–3 km<sup>3</sup> [60]). Third, the crust along the Gondwana 660  
margin, formed primarily through subduction-zone 661  
volcanism and erosion of these volcanic rocks, also has 662  
an appropriate composition to serve as the EM end- 663  
member. More SiO<sub>2</sub>-saturated melts, due to their higher 664  
viscosity and larger volumes, are more likely to stagnate 665  
and differentiate in the crust (and lithospheric mantle), 666  
leading to assimilation during fractional crystallization 667  
(AFC). Because they have lower contents of incompatible 668  
elements, the more saturated melts are also more sensitive 669  
to contamination in the lithosphere. In conclusion, the 670  
composition of the hi-Si group can be explained by 671  
interaction between asthenospheric melts (with composi- 672  
tions intermediate between MORB and HIMU) and a 673  
(EM-type) lithosphere, with variable amounts of litho- 674  
spheric melting being likely. 675

### 3.4. Lithospheric removal model to explain Cenozoic 676 intraplate volcanism on Zealandia 677

A fundamental question concerning the origin of 678  
Cenozoic intraplate volcanism on Zealandia is what causes 679

680 the melting. As noted above, the petrology and geochem-  
 681 istry of the volcanic rocks are consistent with generation of  
 682 the parental melts through decompression melting of  
 683 upwelling asthenosphere combined with lithospheric  
 684 melting to produce the hi-Si melts. The problem is how  
 685 to affix an asthenospheric upwelling to a restricted region  
 686 of the lithosphere, for example Banks Peninsula (~ 50 km  
 687 across) where volcanism persisted for ~6 m.y. or the  
 688 Waiareka–Deborah, Waipiata and Dunedin volcanic  
 689 region (~ 100 km across) where volcanism lasted  
 690 ~ 30 m.y. The plate would have moved  $\geq 300$  km and  
 691  $\geq 1800$  km respectively in the aforementioned time  
 692 intervals. If the upwelling regions were  $\geq 300$  km and  
 693  $\geq 1800$  km respectively, then why is the volcanism not  
 694 regionally more extensive? On the other hand, if the  
 695 upwelling regions had diameters similar to the volcanic  
 696 areas and were fixed in the sublithospheric mantle (similar  
 697 to a plume), why wasn't the volcanism more extensive  
 698 over time and why don't we see any age progressions in  
 699 the volcanism in the direction and at the same rate as plate  
 700 motion?

701 Removal/detachment of parts of the lithospheric keel  
 702 beneath Zealandia can explain how asthenospheric  
 703 upwelling can be localized to specific regions of the  
 704 plate over long periods of time (Fig. 7). In the Dunedin  
 705 region, flexural modeling suggests a thermally weak-  
 706 ened plate, which is interpreted to have resulted from a

707 buoyant load, probably hot asthenosphere, emplaced  
 708 beneath the crust during the mid Miocene [61]. These  
 709 results are consistent with detached lithospheric mantle  
 710 allowing hot asthenosphere to well up to shallow depths  
 711 beneath the Dunedin Volcano when it formed in the mid  
 712 Miocene.

713 Regions of Zealandia's lithospheric keel are inferred to  
 714 contain large amounts of garnet pyroxenite/eclogite (e.g.  
 715 frozen intruded melts and cumulates), as a result of  
 716 magmatic underplating associated with 1) subduction or  
 717 plume volcanism beneath the former Gondwana margin in  
 718 the Mesozoic [27,62] and 2) rifting during separation of  
 719 Zealandia from West Antarctica and Australia (e.g. [2]). It  
 720 has been found for example that lower crustal and mantle  
 721 compositions resulting from arc magmatism can create a  
 722 1–5% density contrast within the normal upper mantle  
 723 [63]. Such density contrasts are sufficient to cause grav-  
 724 itational or Rayleigh–Taylor instabilities, resulting in the  
 725 removal/detachment of the lower lithosphere in a ductile  
 726 manner (e.g. [45,64,65]). This mechanism only requires a  
 727 dense region in the lithosphere that is gravitationally  
 728 unstable and that possesses a rheology conducive to flow  
 729 [66,67]. Modeling results suggest that the latter require-  
 730 ment is easily met at normal lithospheric-mantle rheolo-  
 731 gies and temperatures [65]. Instabilities initiate in response  
 732 to boundary perturbations, and growth rates increase with  
 733 strain rate. Since younger, thinned continental lithosphere

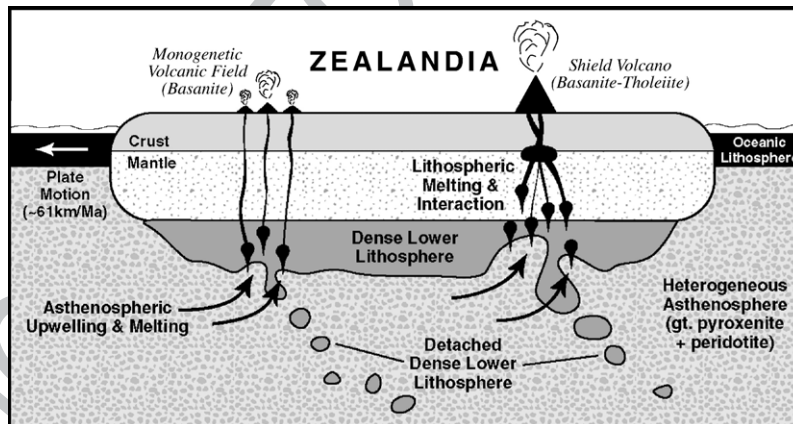


Fig. 7. Lithospheric removal/detachment model for explaining Cenozoic intraplate volcanism on Zealandia. Removal of the cooler, dense lower lithosphere (enriched in eclogite or garnet pyroxenite, e.g. intruded, frozen melts, and/or garnet-rich cumulates) is the result of Rayleigh–Taylor or gravitational instabilities developed along the lithospheric–asthenospheric mantle boundary. Lithospheric stripping is asymmetrical due to the movement of Zealandia lithosphere relative to the asthenospheric mantle. Zealandia is moving west relative to sinking lithospheric instabilities. Clusters of descending dense lower lithosphere may occur beneath areas with long histories of volcanic activity. When relatively small amounts of the lithosphere are removed, garnet pyroxenite/eclogite in hotter upwelling asthenosphere melts to small degrees to form basanitic (and possibly nephelinitic) melts, which form monogenetic volcanic fields (predominantly cinder cones and lava flows). When larger areas of lithospheric mantle are removed, possibly through progressive growth of an instability, larger volumes of asthenosphere upwell to shallower depths, resulting in greater degrees of melting to form alkali basaltic and possibly tholeiitic melts. These melts interact extensively with the lithosphere (possibly both crust and mantle) giving them more enriched trace element and isotopic signatures. Some tholeiites may result directly from lithospheric mantle melting. Areas of greater lithospheric detachment allow greater degrees of melting and the formation shield volcanoes.

734 is most likely to be gravitationally unstable and sink with  
735 respect to the adjacent asthenosphere [65,68], the young  
736 Zealandia lithosphere, thinned and heated in the Late  
737 Cretaceous as a result of continental breakup, is likely to  
738 have been particularly susceptible to the development of  
739 gravitational instabilities. Movement of the low viscosity  
740 Zealandia lithosphere through an anomalously hot upper  
741 mantle [4] at high rates of plate motion during the  
742 Cenozoic would have further enhanced the formation of  
743 gravitational instabilities.

744 The distribution and timing of volcanism can provide  
745 important clues as to the shape and amount of lithosphere  
746 detached by such instabilities, which should detach from  
747 regions of weakness or the top of the region of negative  
748 buoyancy. Since the height of the region that detaches  
749 should be similar to the width of the instability as it sinks,  
750 the surface distribution of volcanism should reflect the  
751 width of the instability and height of the removed litho-  
752 sphere (e.g. [69]). In addition, rapid instability growth and  
753 detachment yield more focused detachment zones (scars)  
754 with greater relief than does slower instability develop-  
755 ment, which favors broad detachment zones with limited  
756 relief along the lithosphere–asthenosphere boundary [45].  
757 For Zealandia, this implies multiple small detachments to  
758 explain scattered low-volumes of low-silica volcanism  
759 such as the Waipiata monogenetic volcanic field. We  
760 suggest that areas of more persistent and larger volume  
761 volcanism (e.g. Dunedin and Banks Peninsula shield  
762 volcanoes) resulted from rapid development of thicker  
763 instabilities. Development of the large Dunedin instability  
764 within the broader Waipiata field may reflect higher  
765 intensities of lithospheric mantle modification (i.e.  
766 addition of dense material) affecting greater lithospheric  
767 thickness beneath the Dunedin volcano than in the  
768 surrounding base of the lithosphere beneath the Waipiata  
769 field. Judging from the volumes and distribution of  
770 Cenozoic magmatism, we infer that lithospheric modifi-  
771 cation was highly heterogenous beneath Zealandia.

772 As a portion of the lithosphere is stripped off and sinks,  
773 asthenosphere can well up into the resulting cavity, melting  
774 by decompression. New volumes of asthenosphere must  
775 have continually upwelled into cavities in the base of the  
776 Zealandia lithosphere as the plate moved over the  
777 asthenosphere at a rate of  $\sim 60$  km/m.y. Therefore decom-  
778 pression melting and volcanism could have continued for  
779 millions to tens of millions of years until the lithosphere  
780 thermally healed itself by conductive cooling. Sequential  
781 detachment of adjacent lithospheric material from an area,  
782 such as Banks Peninsula where Akaroa volcano began  
783 forming as activity at Lyttleton volcano was ending, slows  
784 thermal healing, promotes prolonged volcanism in the area,  
785 and contributes to increasing degrees of melting with time.

786 After a final detachment event, the lithosphere will slowly  
787 anneal, resulting in decreasing degrees of melting and melt  
788 production and increasing degree of Si-undersaturation  
789 with time, as is observed on Banks Peninsula [3].

790 Removal of larger thicknesses of lithospheric mantle  
791 allows asthenosphere to upwell to shallower depths and  
792 over longer vertical distances (reflected in a longer melting  
793 column), to produce larger degrees of partial mantle mel-  
794 ting and thus increased volumes of more SiO<sub>2</sub>-saturated  
795 melts. Increased heat transfer from the upwelling astheno-  
796 sphere to newly exposed parts of the Zealandia lithosphere  
797 will enhance lithospheric melting, resulting in greater  
798 lithospheric contributions to the erupted magmas, in  
799 particular to the largest degree melts (tholeiites) formed  
800 at the top of the melting column. Release of hydrous fluids  
801 through devolatilization and alkali transfer from the  
802 detached metasomatized lithosphere could increase melt-  
803 ing and the production of high silica melts within the  
804 overlying upwelling asthenosphere and within the non-  
805 detached lithosphere. Detached hydrous lithosphere could  
806 also melt as it sinks, providing yet another source for melts  
807 [45]. Devolatilization of detached carbonated lithosphere  
808 could also serve as a source of CO<sub>2</sub> causing the carbonation  
809 of peridotite and eclogite/pyroxenite in the upwelling  
810 asthenosphere above the detaching lithosphere, providing  
811 an additional mechanism for the formation of Si-under-  
812 saturated melts in regions that have undergone a detach-  
813 ment event.

814 In contrast, removal of small thicknesses of litho-  
815 sphere promotes only limited upwelling and thus short-  
816 lived production of small volumes of asthenospheric  
817 melt from a short melting column. Heat transfer from the  
818 upwelling asthenosphere to the base of the overlying  
819 lithosphere and volatile and alkali (+other element)  
820 transfer from the detaching lithosphere to the overlying  
821 asthenosphere and lithosphere will be at a minimum and  
822 thus melts formed from decompression melting of  
823 asthenosphere will have minimal interaction with litho-  
824 spheric components. For volcanic fields such as the  
825 Waipiata, which erupted small volumes of generally  
826 primitive HIMU-type magmas over large areas and long  
827 periods of time, we envisage repeated thin detachments.  
828 It is probable that not all of these thin detachments  
829 produced surface volcanism, with many small-volume  
830 melts instead becoming trapped in the crust [70].

831 In conclusion, the lateral extent of the cavity or  
832 cavities formed by instability growth and detachment  
833 will govern the area of a given volcanic province,  
834 whereas the vertical extent and volume of the cavity will  
835 control the extents and amounts of melting, thereby  
836 influencing the volcanic style: monogenetic volcanic  
837 fields versus composite shield volcanoes. Interruptions

838 to cavity annealing (repeated detachments) may result in  
839 repeated cycles of volcanism at individual shields and  
840 complicated temporal geochemical trends.

#### 841 Acknowledgements

842 We thank D. Rau, J. Sticklus, S. Hauff for analytical  
843 assistance, M. Portnyagin for comments on this manu-  
844 script, and the “Great Plume Debate” Chapman Confer-  
845 ence in Fort William (2005) for talks and discussions that  
846 helped further develop ideas in this paper. We are  
847 especially grateful to Lindy Elkins-Tanton and Kurt Panter  
848 for constructive reviews which helped to improve this  
849 manuscript significantly. We acknowledge Otago Univer-  
850 sity for providing KH with the William Evans Fellowship,  
851 during which this project was initiated, and the German  
852 Research Foundation (DFG Project HO1833/12-1, New  
853 Zealand Volcanism) for funding part of this project. JW  
854 acknowledges support from the New Zealand FRST via  
855 contract C05X0006.

#### 856 Appendix A. Supplementary data

857 Supplementary data associated with this article  
858 can be found, in the online version, at [doi:10.1016/j.](https://doi.org/10.1016/j.epsl.2006.06.001)  
859 [epsl.2006.06.001](https://doi.org/10.1016/j.epsl.2006.06.001).

#### 860 References

- 861 [1] W.J. Morgan, Convection plumes in the lower mantle, *Nature*  
862 230 (1971) 42–43.  
863 [2] S.D. Weaver, I.E.M. Smith, New Zealand intraplate volcanism,  
864 in: R.W. Johnson, J. Knutson, S.R. Taylor (Eds.), *Intraplate*  
865 *Volcanism in Eastern Australia and New Zealand* Chapter 4,  
866 Cambridge University Press, 1989, pp. 157–188.  
867 [3] R.J. Sewell, S.D. Weaver, M.B. Reay, *Geology of Banks*  
868 *Peninsula. Scale 1:100 000. Institute of Geological and Nuclear*  
869 *Sciences geological map 3, 1 sheet, Institute of Geological and*  
870 *Nuclear Sciences Ltd, Lower Hutt, New Zealand (1992).*  
871 [4] C.A. Finn, R.D. Mueller, K.S. Panter, A Cenozoic diffuse  
872 alkaline magmatic province (DAMP) in the southwest Pacific  
873 without rift or plume origin, *Geochem. Geophys. Geosyst.* 6  
874 (2005) Q02005, [doi:10.1029/2004GC000723](https://doi.org/10.1029/2004GC000723).  
875 [5] L. Hoke, R. Poreda, A. Reay, D. Weaver, The subcontinental  
876 mantle beneath southern New Zealand, characterized by helium  
877 isotopes in intraplate basalts and gas-rich springs, *Geochim.*  
878 *Cosmochim. Acta* 64 (2000) 2489–2507.  
879 [6] C.J. Adams, Migration of late Cenozoic volcanism in the South  
880 Island of New Zealand and the Campbell Plateau, *Nature* 294  
881 (1981) 153–154.  
882 [7] E. Farrar, J.M. Dixon, Overriding of the Indian–Antarctic ridge:  
883 origin of the Emerald Basin and migration of late Cenozoic  
884 volcanism in southern New Zealand and Campbell Plateau,  
885 *Tectonophysics* 104 (1984) 243–256.  
886 [8] D.C.R. Coombs, Y. Kawachi, C.A. Landis, W.F. McDonough,  
887 A. Reay, Cenozoic volcanism in north, east, and central Otago,

- in: I.E.M. Smith (Ed.), *Late Cenozoic Volcanism in New Zealand*,  
Bulletin, vol. 23, Royal Society of New Zealand, 1986,  
pp. 278–312. 888  
889  
890 [9] S.R. Hart, J. Blusztajn, W.E. LeMasurier, D.C. Rex, Hobbs Coast  
891 Cenozoic volcanism: implications for the West Antarctic rift  
892 system, *Chem. Geol.* 139 (1997) 223–248. 893  
894 [10] K.S. Panter, S.R. Hart, P. Kyle, J. Blusztajn, T. Wilch, Geo-  
895 chemistry of Late Cenozoic basalts from the Crazy Mountains:  
896 characterization of mantle sources in Marie Byrd Land, Antarctica,  
897 *Chem. Geol.* 165 (2000) 215–241. 898  
899 [11] C. Cook, R.M. Briggs, I.E.M. Smith, R. Maas, Petrology and  
900 geochemistry of intraplate basalts in the South Auckland  
901 Volcanic Field, New Zealand: evidence for two coeval magma  
902 suites from distinct sources, *J. Petrol.* 46 (2005) 473–503. 901  
902 [12] K.S. Panter, J. Blusztajn, S.R. Hart, P.R. Kyle, R. Esser, W.C.  
903 McIntosh, The origin of HIMU in the SW Pacific: evidence from  
904 intraplate volcanism in Southern New Zealand and subantarctic  
905 islands, *J. Petrol.* (2006) 1–32, [doi:10.1093/petrology/egl024](https://doi.org/10.1093/petrology/egl024). 905  
906 [13] E.J. Dasch, A.L. Evans, E. Essene, Radiometric and petrolog-  
907 ic data from eclogites and megacrysts of the Kakanui Mineral  
908 Breccia, New Zealand, *Geol. Soc. Am. Abstr. Progr.* 7 (1970)  
909 532–533. 910  
911 [14] I. McDougall, D.S. Coombs, Potassium–argon for the Dunedin  
912 volcano and outlying volcanics, *N.Z. J. Geol. Geophys.* 16  
913 (1973) 179–188. 912  
914 [15] C.J. Adams, A.F. Cooper, K–Ar age of lamprophyre dike swarm  
915 near Lake Wanaka, west Otago, South Island, New Zealand, *N.Z.*  
916 *J. Geol. Geophys.* 39 (1996) 17–23. 913  
917 [16] A.F. Cooper, B.A. Barreiro, D.L. Kimbrough, J.M. Mattinson,  
918 Lamprophyre dike intrusion and the age of the Alpine Fault, *New*  
919 *Zealand, Geology* 15 (1987) 941–944. 917  
920 [17] W.H. Matthews, G.H. Curtis, Date of the Pliocene–Pleistocene  
921 boundary in New Zealand, *Nature* 212 (1966) 979–980. 920  
922 [18] J.B. Wright, Contributions to the volcanic succession and  
923 petrology of the Auckland Islands. II. Upper parts of the Ross  
924 Volcano, *Transactions of the Royal Society of New Zealand,*  
925 *Geology* 5 (1967) 71–87. 922  
926 [19] J.B. Wright, Contributions to the volcanic succession and  
927 petrology of the Auckland Islands. V. Chemical analyses from  
928 the upper parts of the Ross Volcano, including minor intrusions,  
929 *J. R. Soc. N.Z.* 1 (1967) 175–183. 926  
930 [20] C.J. Adams, Age of the volcanoes and granite basement of the  
931 Auckland Islands, Southwest Pacific, *N.Z. J. Geol. Geophys.* 26  
932 (1983) 227–237. 930  
933 [21] C.J. Adams, P.A. Morris, J.M. Beggs, Age and correlation of  
934 volcanic rocks of Campbell Island and metamorphic basement of  
935 the Campbell Plateau, southwest Pacific, *N.Z. J. Geol. Geophys.*  
936 22 (1979) 679–691. 933  
937 [22] R.W. Le Maitre, P. Bateman, A. Dudek, J. Keller, J. Lameyre, M.J.  
938 Le Bas, P.A. Sabine, R. Schmid, H. Sorenson, A. Streckeisen,  
939 A.R. Woolley, B. Zanettin, *A Classification of Igneous Rocks*  
940 and Glossary of Terms: Recommendations of the International  
941 Union of Geological Sciences Subcommittee on the Systematics  
942 of Igneous Rocks, Blackwell, Oxford, 1989. 193 pp. 941  
943 [23] S.D. Weaver, R.J. Pankhurst, A precise Rb–Sr age for the  
944 Mandamus Igneous Complex, North Canterbury, and regional  
945 tectonic implications, *N.Z. J. Geol. Geophys.* 34 (1991) 341–345. 943  
946 [24] J.A. Baker, J.A. Gamble, I.J. Graham, The age, geology and  
947 geochemistry of the Tapuaenuku Igneous Complex, Marlbor-  
948 ough, New Zealand, *N.Z. J. Geol. Geophys.* 37 (1994) 249–268. 946  
949 [25] G.W. Grindley, C.J.D. Adams, J.T. Lumb, W.A. Watters,  
950 Paleomagnetism, K–Ar dating and tectonic interpretation of 949



- 950 Upper Cretaceous and Cenozoic volcanic rocks of the Chatham  
951 Islands, New Zealand, *N.Z. J. Geol. Geophys.* 20 (1977)  
952 425–467.
- 953 [26] V.E. Tappenden, Magmatic response to the evolving New  
954 Zealand margin of Gondwana during the Mid-Late Cretaceous,  
955 PhD thesis, University of Canterbury, 2003.
- 956 [27] B.C. Storey, P.T. Leat, S.D. Weaver, R.J. Pankhurst, J.D.  
957 Bradshaw, S. Kelley, Mantle plumes and Antarctica–New  
958 Zealand rifting: evidence from mid-Cretaceous mafic dykes, *J.*  
959 *Geol. Soc. (Lond.)* 156 (1999) 659–671.
- 960 [28] R.J. Sewell, S. Nathan, Geochemistry of Late Cretaceous and  
961 Early Tertiary basalts from south Westland, *N.Z. Geol. Surv.*  
962 *Record* 18 (1987) 87–94.
- 963 [29] C.J. Phillips, A.F. Cooper, J.M. Palin, S. Nathan, Geochrono-  
964 logical constraints on Cretaceous–Paleocene volcanism in South  
965 Westland, New Zealand, *N.Z. J. Geol. Geophys.* 48 (2005) 1–14.
- 966 [30] C.A. Landis, D.S. Coombs, Metamorphic belts and orogenesis in  
967 Southern New Zealand, *Tectonophysics* 4 (1967) 501–518.
- 968 [31] R. Sutherland, Basement geology and tectonic development of  
969 the greater New Zealand region: an interpretation from regional  
970 magnetic data, *Tectonophysics* 308 (1999) 341–362.
- 971 [32] D.R. Gregg, Sheet 18 Hurunui, Geological Map of New Zealand  
972 1:250 000, New Zealand Department of Scientific and Industrial  
973 Research, 1964.
- 974 [33] R.J. Sewell, I.L. Gibson, Petrology and geochemistry of Tertiary  
975 volcanic rocks from inland Central and South Canterbury, South  
976 Island, New Zealand, *N.Z. J. Geol. Geophys.* 31 (1988) 477–492.
- 977 [34] J.A. Gamble, P.A. Morris, C.J. Adams, The geology, petrology  
978 and geochemistry of Cenozoic volcanic rocks from the Campbell  
979 Plateau and Chatham Rise, in: I.E.M. Smith (Ed.), *Late Cenozoic*  
980 *Volcanism in New Zealand*, Bulletin, vol. 23, Royal Society of  
981 New Zealand, 1986, pp. 344–365.
- 982 [35] J.C. Schofield, Distribution of Lower Oligocene Volcanics in  
983 New Zealand, *N.Z. J. Sci. Technol.* B33 (3) (1951) 201–217.
- 984 [36] J. Morris, The stratigraphy of the Amuri Limestone group, east  
985 Marlborough, Unpublished PhD thesis, University of Canter-  
986 bury, 1987.
- 987 [37] J.M. McLennan, S.D. Weaver, Olivine–nephelinite at Mounseys  
988 Creek, Oxford, Canterbury, N.Z. *J. Geol. Geophys.* 27 (1984)  
989 389–390.
- 990 [38] A.F. Cooper, A carbonatitic lamprophyre dike swarm from the  
991 Southern Alps, Otago and Westland, in: I.E.M. Smith (Ed.), *Late*  
992 *Cenozoic Volcanism in New Zealand*, Bulletin, vol. 23, Royal  
993 Society of New Zealand, 1986, pp. 278–312.
- 994 [39] J.A. Gamble, C.J. Adams, Volcanic geology of Carnley volcano,  
995 Auckland Islands, *N.Z. J. Geol. Geophys.* 28 (1985) 43–54.
- 996 [40] J.J. Stipp, I. Mc Dougall, Geochronology of the Banks Peninsula  
997 volcanoes, New Zealand, *N.Z. J. Geol. Geophys.* 11 (1968)  
998 1239–1260.
- 999 [41] D.J. Cullen, Quaternary volcanism at the Antipodes Islands: its  
1000 bearing on the structural interpretation of the southwest Pacific, *J.*  
1001 *Geophys. Res.* 74 (1969) 4213–4220.
- 1002 [42] R. Sutherland, The Australia–Pacific boundary and Cenozoic  
1003 plate motions in the SW Pacific — some constraints from Geosat  
1004 data, *Tectonics* 14 (1995) 819–831.
- 1005 [43] V. Clouard, A. Bonneville, Ages of seamounts, slands and  
1006 plateaus and plateaus on the Pacific plate, in: G.R. Foulger, J.H.  
1007 Natland, D.C. Presnall, D.L. Anderson (Eds.), *Plates, Plumes,*  
1008 *and Paradigms*, Geological Society of America Special Paper,  
1009 vol. 388, Geological Society of America, 2005, pp. 71–90.
- 1010 [44] W.I. Reilly, Gravitational expression of the Dunedin Volcano,  
1011 *N.Z. J. Geol. Geophys.* 15 (1971) 16–21.
- [45] L.T. Elkins-Tanton, Continental magmatism caused by litho-  
spheric delamination, in: G.R. Foulger, J.H. Natland, D.C.  
Presnall, D.L. Anderson (Eds.), *Plates, Plumes, and Paradigms*,  
Geological Society of America Special Paper, vol. 388,  
Geological Society of America, 2005, pp. 449–461.
- [46] K. Hirose, I. Kushiro, Partial melting of dry peridotites at high  
pressures: determination of compositions of melts segregated  
from peridotite using aggregates of diamond, *Earth Planet. Sci.*  
*Lett.* 114 (1993) 477–489.
- [47] K. Hirose, Partial melt compositions of carbonated peridotite at  
3 GPa and role of CO<sub>2</sub> in alkali-basalt magma generation,  
*Geophys. Res. Lett.* 24 (1997) 2837–2840.
- [48] T. Kogiso, K. Hirose, E. Takahashi, Melting experiments on  
homogeneous mixtures of peridotite and basalt: application to the  
genesis of ocean island basalt, *Earth Planet. Sci. Lett.* 162 (1998)  
45–61.
- [49] T. Kogiso, M.M. Hirschmann, D.J. Frost, High-pressure partial  
melting of garnet pyroxenite: possible mafic lithologies in the  
source of ocean island basalts, *Earth Planet. Sci. Lett.* 216 (2003)  
603–617.
- [50] M.M. Hirschmann, T. Kogiso, M.B. Baker, E.M. Stolper, Alkalic  
magmas generated by partial melting of garnet pyroxenite,  
*Geology* 31 (2003) 481–484.
- [51] R. Dasgupta, M.M. Hirschmann, K. Stalker, Immiscible transition  
from carbonate-rich to silicate-rich melts in the 3 GPa melting  
interval of eclogite+CO<sub>2</sub> and genesis of silica-undersaturated  
ocean island lavas, *J. Petrol.* 47 (2006) 647–671.
- [52] E.M. Klein, C.H. Langmuir, Global correlations of ocean ridge  
basalt chemistry with axial depth and crustal thickness, *J.*  
*Geophys. Res.* 92 (1987) 8089–8115.
- [53] M. Pertermann, M.M. Hirschmann, K. Hametner, D. Guenther,  
M.W. Schmidt, Experimental determination of trace element  
partitioning between garnet and silica-rich liquid during anhy-  
drous partial melting of MORB-like eclogite, *Geochem. Geo-*  
*phys. Geosyst.* 5 (2004) Q05A01, doi:10.1029/2003GC000638.
- [54] S. Klemme, J.D. Blundy, B. Wood, Experimental constraints of  
major and trace element partitioning during partial melting of  
eclogite, *Geochim. Cosmochim. Acta* 66 (2002) 3109–3123.
- [55] C. Chauvel, A.W. Hofmann, P. Vidal, HIMU-EM: the French  
Polynesian connection, *Earth Planet. Sci. Lett.* 110 (1992)  
99–119.
- [56] M.M. Hirschmann, E.M. Stolper, A possible role for garnet  
pyroxenite in the origin of the “garnet signature” in MORB,  
*Contrib. Mineral. Petrol.* 124 (1996) 185–208.
- [57] R. Dasgupta, M.M. Hirschmann, N. Dellas, The effect of bulk  
composition on the solidus of carbonated eclogite from partial  
melting experiments at 3 GPa, *Contrib. Mineral. Petrol.* 149  
(2005) 288–305.
- [58] T.J. Falloon, L.V. Danyushevsky, D.H. Green, Peridotite melting  
at 1 GPa: reversal experiments on partial melt compositions  
produced by peridotite–basalt sandwich experiments, *J. Petrol.*  
42 (2001) 2363–2390.
- [59] C.C. Lundstrom, K. Hoernle, J. Gill, U-series disequilibria in  
volcanic rocks from the Canary Islands: plume versus lithospheric  
melting, *Geochim. Cosmochim. Acta* 67 (2003) 4153–4177.
- [60] J.C. Carracedo, E.R. Badiola, V. Soler, The 1730–1736 eruption  
of Lanzarote, Canary Islands: a long high-magnitude basal-  
saltic fissure eruption, *J. Volcanol. Geotherm. Res.* 53 (1992)  
239–250.
- [61] N.J. Godfrey, F. Davey, T.A. Stern, D. Okaya, Crustal structure  
and thermal anomalies of the Dunedin Region, South Island,  
New Zealand, *J. Geophys. Res.* 106 (2001) 30,835–830,848.

- 1074 [62] S.D. Weaver, B.C. Storey, R.J. Pankhurst, S.B. Mukasa, V.J.  
1075 DiVenere, J.D. Bradshaw, Antarctica–New Zealand rifting  
1076 and Marie Byrd Land lithospheric magmatism linked to ridge  
1077 subduction and mantle plume activity, *Geology* 22 (1994)  
1078 811–814.
- 1079 [63] M. Jull, P.B. Kelemen, On conditions for lower crustal convective  
1080 instability, *J. Geophys. Res.* 106 (2001) 6423–6446.
- 1081 [64] G.A. Houseman, D.P. McKenzie, P. Molnar, Convective insta-  
1082 bility of a thickened boundary layer and its relevance for the  
1083 thermal evolution of continental convergent belts, *J. Geophys.*  
1084 *Res.* 86 (1981) 6115–6132.
- 1085 [65] L.T. Elkins-Tanton, Continental magmatism, volatile recycling,  
1086 and a heterogeneous mantle caused by lithospheric Rayleigh-  
1087 Taylor instabilities, *J. Geophys. Res.* (in revision).
- 1088 [66] B. Schott, D.A. Yuen, H. Schmeling, The significance of shear  
1089 heating in continental delamination, *Phys. Earth Planet. Inter.* 118  
1090 (2000) 273–290.
- 1091 [67] L.T. Elkins-Tanton, B.H. Hager, Melt intrusion as a trigger for  
1092 lithospheric foundering and the eruption of the Siberian flood  
1093 basalt, *Geophys. Res. Lett.* 27 (2000) 3937–3940.
- 1094 [68] Y.H. Poudjom Djomani, S.Y. O’Reilly, W.L. Griffin, P. Morgan,  
1095 The density structure of subcontinental lithosphere through time,  
1096 *Earth Planet. Sci. Lett.* 184 (2001) 605–621.  
1119
- [69] D.L. Turcotte, G. Schubert, *Geodynamics*, Cambridge University  
Press, Cambridge, England, 2002. 456 pp. 1097 1098
- [70] K. Nemeth, J.D.L. White, A. Reay, U. Martin, Compositional  
variation during monogenetic volcano growth and its implica-  
tions for magma supply to continental volcanic fields, *J. Geol.*  
*Soc. ( Lond. )* 160 (2003) 523–530. 1099 1100 1101 1102
- [71] W.H.F. Smith, D.T. Sandwell, Global seafloor topography from  
satellite altimetry and ship depth soundings, *Science* 277 (1997)  
1957–1962. 1103 1104 1105
- [72] S.-S. Sun, W.F. McDonough, Chemical and isotopic system-  
atics of oceanic basalts: implications for mantle composi-  
tion and processes, in: A.D. Saunders, M.J. Norry (Eds.),  
*Magmatism in the Ocean Basins*, Geological Society Lon-  
don Special Publication, vol. 42, Blackwell, London, 1989,  
pp. 313–345. 1106 1107 1108 1109 1110 1111
- [73] A.W. Hofmann, Chemical differentiation of the Earth: the  
relationship between mantle, continental and oceanic crust,  
*Earth Planet. Sci. Lett.* 90 (1988) 297–314. 1112 1113 1114
- [74] R.C. Price, A.F. Cooper, J.D. Woodhead, I.A.N. Cartwright,  
Phonolitic diatremes within the Dunedin Volcano, South Island,  
New Zealand, *J. Petrol.* 44 (2003) 2053–2080. 1115 1116 1117 1118